

Università degli Studi di Napoli Federico II

Scuola Politecnica e delle Scienze di Base
Corso di Laurea Magistrale in Ingegneria Aerospaziale

TESI DI LAUREA MAGISTRALE
IN
INGEGNERIA AEROSPAZIALE

Development of a Java-Based Framework for Aircraft Preliminary Design

Wing Aerodynamic Analysis Module,
Aircraft Longitudinal Static Stability Module

Relatori:

Prof. Ing. Fabrizio Nicolosi
Prof. Ing. Agostino De Marco

Candidato:

Manuela Ruocco
Matricola M53/408

Dedica

ABSTRACT

The purpose of this Thesis work is to introduce the features and the potentiality of ADOpt (*Aircraft Design and Optimization Tool*), a java-based framework concieved as a fast and efficient tool useful as support in the preliminary design phases of an aircraft, and during its optimizaton process.

The ADOpt development originates in the Departement of Industrial Engineering of University of Naples “Federico II”, where is still in development. At present this tool is capable to perform a multi-disciplinary analysis of an aircraft whose data can be entered by the user, with an XML, or loaded into memory. The ultimate goal of ADOpt is to carry out an optimization process where the analysis are cyclically repeated in order to optimize some parameters while keeping others in fixed limits. Currently the software is able to esimate the aircraft weight breakdown, the center of gravity location, calculate some aerodynamic parameters and estimate the performance. All these types of estimates can be usually performed using several interchangeable analysis methods, comparable and interchangeable. It is also provided a static longitudinal stability analysis, take-off and landing performances and the generation of Payload Range chart.

ADOpt can be used from the command line or with a dedicated graphical user interface (GUI). The GUI allows the user to have an immediate feedback about the aircraft features when changing the input parameters, to manage multiple aircraft simultaneously and compare them side by side, and to view a 3D CAD model of the aircraft.

The ADOpt potentiality, in the world of research or in industry, are remarkable and the software strengths are a considerable computing speed and flexibility, with an user-friendly GUI.

The structure of this thesis work has as ultimate goal to provide a comprehensive overview about ADOpt and, at the same time, it is intended to be a developer’s manual. The first chapters provide a complete software overview paying particular attention at actual features and future goals. Following chapters introduce some case of study and the results achieved. At the beginning of each chapter is exposed the theoretical background, afterwards there is a description of the Java architecture and, at the end is reported the Test class used for the analysis and its results.

SOMMARIO

Lo scopo che il presente lavoro di Tesi auspica raggiungere è quello di presentare le capacità possedute e le potenzialità future di ADOpT, un software scritto in Java che si configura come uno strumento veloce ed efficiente per il supporto nella fase di progetto preliminare di un velivolo e per la sua ottimizzazione.

Lo sviluppo di ADOpT (*Aircraft Design and Optimization Tool*) nasce all' interno del Dipartimento di Ingegneria Industriale dell' Università degli Studi di Napoli Federico II, ove è tutt'ora in fase di progresso. Il software è attualmente in grado di svolgere una parziale analisi multi-disciplinare di un velivolo i cui dati sono immessi dall' utente tramite XML o caricati in memoria. La linea guida dello sviluppo del software porta verso l' implementazione di un processo di ottimizzazione nel quale le analisi sono ciclicamente ripetute al fine di ottimizzare alcuni parametri mantenendone altri all' interno di limiti imposti.

Attualmente ADOpT è in grado di effettuare una completa stima dei pesi, valutare la posizione del baricentro, calcolare un notevole numero di parametri aerodinamici e caratteristiche di performance. La stima di ciascun parametro può essere effettuata tramite diversi metodi implementati, tra di loro confrontabili ed intercambiabili. Inoltre è prevista un' analisi di stabilità statica, prestazioni di decollo ed atterraggio e la generazione del diagramma *Payload Range*.

ADOpT può essere utilizzato sia in modalità *batch*, ossia da riga di comando, che tramite interfaccia grafica. Tale duplice scelta consente di ottenere le migliori prestazioni sia nei processi di analisi, ove la GUI consente di avere un immediato riscontro grafico, sia nei processi di ottimizzazione.

Dunque le potenzialità di ADOpT nel mondo della ricerca od anche in quello industriale sono senza dubbio notevoli e il software gioca i suoi punti di forza in un' elevata flessibilità e una notevole rapidità di calcolo, senza dimenticare una *user-friendly* interfaccia grafica.

L' organizzazione di questo lavoro di Tesi è stata studiata per cercare di fornire una completezza di esposizione, ma allo stesso tempo risultare un utile manuale per lo sviluppatore. I primi capitoli forniscono una visione globale del software con particolare attenzione alle funzionalità presenti e alle scelte effettuate. I capitoli che seguono presentano una panoramica su alcune funzionalità di ADOpT con i relativi casi di studio e i risultati ottenuti dalle analisi. Per ogni capitolo viene preliminarmente fornita una visione globale circa la teoria alla base dei metodi implementati, seguita dalla descrizione delle classi e dei metodi relativi in Java ed è, infine, riportato il codice della *Test Class* implementata per lo svolgimento delle analisi con i relativi risultati.

Contents

I Aircraft Design Overview	1
1 Aircraft Design	2
2 ADOpt application overview	3
II Development of Application	4
3 Introduction to Java	5
4 Work Object	6
4.1 Introduction	6
4.2 Input data from .XML file	6
4.3 Default Aircraft	7
4.3.1 How is made a default Aircraft	8
4.3.2 How is made a default Wing	11
4.4 Database in JPAD	12
4.4.1 Setup database	13
4.4.2 Assign database using an Aircraft object	13
4.4.3 Assign database using a Wing object	13
4.4.4 User's guide	14
III Functionality Overview	16
5 Work Object Data	17
6 Wing Lift Characteristics	18
6.1 Theoretical background	18
6.1.1 Zero-Lift Angle and Lift Coefficient Slope	19
6.1.2 End of Linearity angle of attack	20
6.1.3 Maximum Lift Coefficient	20
6.1.4 Stall Angle of Attack	23
6.1.5 Construction of the curve	23
6.1.6 Mach number effects on Lift curve	24
6.1.7 High Lift devices	25
6.2 Java Class Architecture	26
6.3 Case Study	26

7 Wing Drag Characteristics	27
7.1 Theoretical background	29
7.2 Java Class Architecture	29
7.3 Case Study	30
8 Downwash Estimation	32
8.1 Theoretical background	32
8.2 Java Class Architecture	34
8.2.1 Constant Downwash Gradient	35
8.2.2 Variable Downwash Gradient	36
8.3 Case Study	38
9 Aircraft Longitudinal Static Stability	41
9.1 Aerodynamic Lift	43
9.1.1 Wing	44
9.1.2 Fuselage	44
9.1.3 Horizontal Tail	46
9.1.4 Complete Aircraft	48
9.2 Aerodynamic Drag	48
9.2.1 Drag of a lifting surface	49
9.2.2 Additional drag due to elevator	49
9.3 Pitching Moments	50
9.3.1 Lifting surface	51
9.3.2 Fuselage	52
9.4 Propulsors	56
9.4.1 Stability Calculation	56
9.4.2 Neutral Point and Static Margin	56
9.5 Java Class Architecture	56
9.6 Case Study	56
10 Minor Works	57
Appendices	
A HDF dataset and database reader creation	59
A.1 Chart Digitization	59
A.2 Creation of an HDF file with Matlab	60
B App2	63
Glossary	65
Acronyms	67
List of symbols	68
Bibliography	70

Part I

Aircraft Design Overview

Chapter **1**

Aircraft Design

Chapter 2

ADOpT application overview

Part II

Development of Application

Chapter 3

Introduction to Java

Chapter 4

Work Object

*Citazione
citazione
– Autore*

4.1 Introduction

In JPAD it is possible to read an .XML file as input or generate an object whose data are written in the code. Both in the first and in the second case all needed variables are initialized with data relating the chosen aircraft. The difference between these two methods is that using an .XML file, user can define its own aircraft having a clear view about the needed data useful for the analysis.

Contrariwise in order to perform test of program functionality, to use a default aircraft is the most simple way to generate a work object.

4.2 Input data from .XML file

XML is a file extension for an *Extensible Markup Language (XML)* file format used to create common information formats and share both the format and the data on the World Wide Web, intranets, and elsewhere using standard ASCII text. It is defined “Markup Language” due to the use of tags that describes the content. XML is considered extensible because the markup symbols are unlimited and self-defining. So it is possible to use a personal tag for each data. In this way to read an .XML file results relatively simple.[10]

The key concepts of an .XML File Format are the followings:

- markup symbol (tag)
- attribute
- tree structure

As mentioned, each part of the test is contained between an opening **markup symbol** and an end markup symbol that expressed the meaning of the text.

```
<name>Test XML</name>
```

Figure 4.1: Use of markup symbols in XML language.

In addition to tag name, the markup symbols may contain also some **attributes** that introduce more informations such as the unit of measure.

```
<tag attribute1='value' attribute2='value'> text </tag>
```

Figure 4.2: Use of attributes in XML language.

An .XML file has a tree structure where there are external knots that branch into internal knots.

In order to read an XML file it is necessary, first of all, to give the file path. The class JPADXmlReader opens the file and the methods of the class MyXMLReaderUtils reads the useful data from the XML having the tag path as input. It is possible to read data as Amount, namely with units of measurement or as double. The unit of measurement is written in the attributes of data in XML file.

Likewise it is possible to write output data on XML file using JPADDaWriter class. First of all it is necessary to define and build the xml tree structure. After each variable is associated with a name that is the markup symbol of the XML file.

4.3 Default Aircraft

Actually it is possible to define two different aircraft in order to test the functionality of the application: **ATR-72** and **B747-100B**.

The **ATR 72** is a twin-engine turboprop made by the French-Italian aircraft manufacturer ATR entered service in 1989. It was developed as a variant of the ATR 42 with a 4.5 m stretched fuselage. The ATR 72 was developed from the ATR 42 in order to increase the seating capacity (48 to 66 in standard configuration) by stretching the fuselage, increasing the wingspan, adding more powerful engines, and increasing fuel capacity by approximately 10 percent.[6] It has been typically employed as a regional airliner, although other roles have been performed by the type such as corporate transport, cargo aircraft and maritime patrol aircraft. [5]

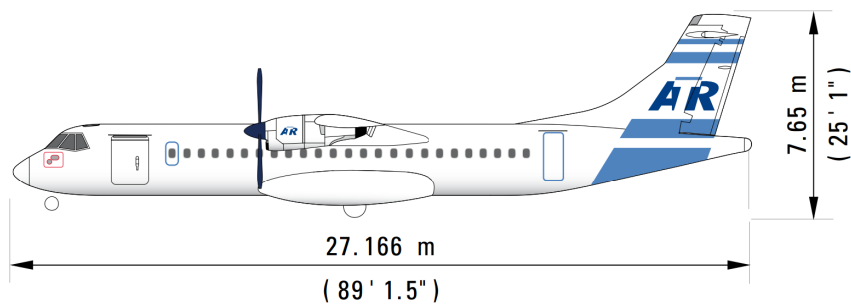


Figure 4.3: ATR 72. Side view.

The **Boeing 747-100B** is a four-engined long-range widebody commercial jet airliner and cargo aircraft produced by the American manufacturer Boeing Commercial Airplanes. It has a capacity of maximum 480 passengers in a partial double deck configuration. The Boeing 747 It is also known as Jumbo Jet. The basic B747-100 entered service with Pan American On January 15, 1970.

One of the reasons to create the 747 was reductions in airfares with a consequent increase of passenger traffic[7]. The original version of the 747 had two and a half times greater capacity than the Boeing 707, one of the common large commercial aircraft of the 1960s and it was the largest passenger carrier from 1970 until the introduction of Airbus A380.[8] The Boeing 747 had two aisles and four wing-mounted engines. The upper deck is its distinctive "hump" along the forward part of the aircraft. It provides space for a lounge or extra seating. The raised cockpit allows front loading of cargo on freight variants.

The 747-100B model was developed from the 747-100SR. This configuration had a typical 452 passengers and unlike the original 747-100, the 747-100B was offered with Pratt & Whitney JT9D-7A, General Electric CF6-50, or Rolls-Royce RB211-524 turbofan engines.

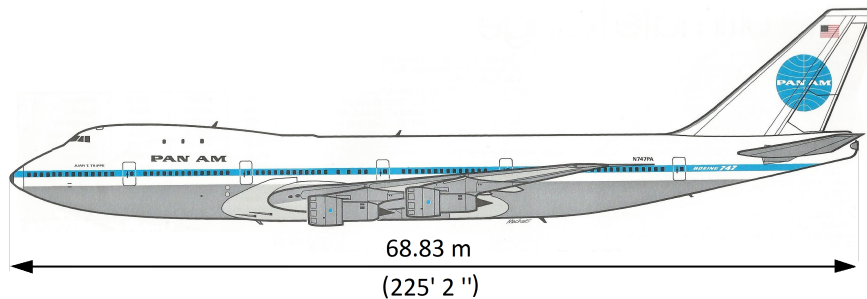


Figure 4.4: Boeing 747-100B. Side view.

4.3.1 How is made a default Aircraft

In order to define a Default Aircraft in a test class, and use it to check the functionalities of the application, it is necessary to follow some step. First of all it is necessary to initialize the working directory tree using the method `initWorkingDirectoryTree` of `MyConfiguration` class located in `JPADConfigs` package that initializes the working directory tree and fill the map of folders. This step is required in order to create the following default folders that are necessary for the right behavior of the code:

- Database directory
- Input directory
- Output directory

Using `MyConfiguration` class it's possible to point at a specific folder, like the input or output directory, with the static method `getDir`. This is a crucial step that must be executed at the beginning of every test. To set the working directory with the useful folders, it's necessary to call the function `initWorkingDirectoryTree()` at the beginning of each test. The function creates all necessary folders. Moreover the function has been overloaded and it can be even called with a variable number of arguments (`initWorkingDirectoryTree(String...str)`). These strings are the directory strings in `MyConfiguration` class. After it is possible to create an `Aircraft` object choosing between "ATR-72" or "B747-100B" using the method `createDefaultAircraft` from `Aircraft` class. This method defines a new `Aircraft` object and invokes another `Aircraft`'s method that creates the components using default data. In the method `createDefaultAircraft` there is a calling to the builder of `Aircraft` class that initializes the objects of the classes that perform calculations. At this step all the components of the aircraft are created. It is possible also to define new airfoils for the aircraft or change some data from the existing.

Afterwards it is necessary to set the operating conditions such as the number of Mach of

analysis or altitude. Each default aircraft has a set of default conditions but the user could change them.

In order to manage all the aircraft related analysis it is necessary to define an object of the class ACAnalysisManager. Similarly to the aircraft, exist an analysis manager also for the wing that is an object of the LSAerodynamicAnalysis class.

The next step is to define and assign the needed databases. This will be explained in detail in the next section. Finally it is possible to do analysis.

Listing 4.1 Generation of default aircraft

```
public static void main(String[] args) {

    // -----
    // Define directory
    // -----
    MyConfiguration.initWorkingDirectoryTree();

    // -----
    // Generate default Aircraft
    // -----
    Aircraft aircraft = Aircraft.createDefaultAircraft("B747-100B");
    LiftingSurface theWing = aircraft.get_wing();

    // Default operating conditions
    OperatingConditions theConditions = new OperatingConditions();

    // -----
    // Define an ACAnalysisManager Object
    // -----
    ACAnalysisManager theAnalysis = new ACAnalysisManager(theConditions);
    theAnalysis.updateGeometry(aircraft);

    // -----
    // Define an LSAerodynamicsManager Object
    // -----
    LSAerodynamicsManager theLSAnalysis = new LSAerodynamicsManager (
        theConditions,
        theWing,
        aircraft
    );

    // -----
    // Setup database(s)
    // -----

    theLSAnalysis.setDatabaseReaders(
        new Pair(DatabaseReaderEnum.AERODYNAMIC,
            "Aerodynamic_Database_Ultimate.h5"),
        new Pair(DatabaseReaderEnum.HIGHLIFT,
            "HighLiftDatabase.h5")
    );

    // -----
    // Do analysis
    // -----
    theAnalysis.doAnalysis(aircraft,
        AnalysisTypeEnum.AERODYNAMIC);
}
```

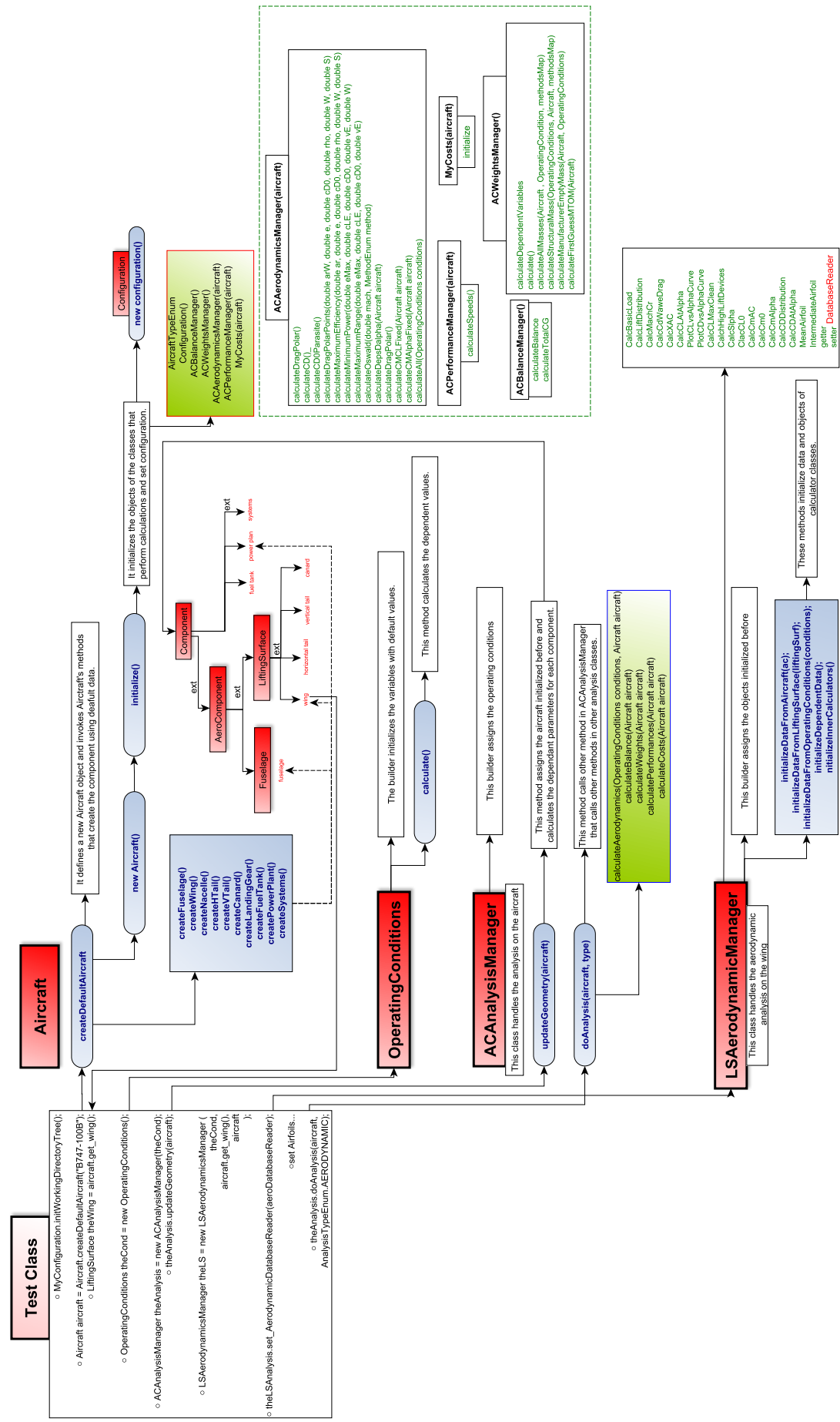


Figure 4.5: Flow chart of the creation of default Aircraft.

4.3.2 How is made a default Wing

Similary to the default aircraft it is possible to define a default wing. This is very useful if the user wants to make an analysis only on a wing. In this case it is necessary to define the origin of the **Local Reference Frame (LRF)** in **Body Reference Frame (BRF)** and the coordinates of the **Gravity Center (GC)**.

Contrary to the case of the aircraft, for an isolated wing there isn't necessary to define a fuselage in order to create a **Lifting Surface** object, but there is an overload of the builder that doesn't need a fuselage as input. In this case the exposed surface is calculated as the surface of the wing.

Listing 4.2 Generation of an isolated Wing

```
public static void main(String[] args) {

    // Assign all default folders
    MyConfiguration.initWorkingDirectoryTree();

    // -----
    // Coordinates of LRF
    // -----

    double xAw = 11.0; //meter
    double yAw = 0.0;
    double zAw = 1.6;
    double iw = 0.0;

    // -----
    // Generate default Wing
    // -----

    LiftingSurface theWing = new LiftingSurface(
        "Wing", // name
        "Data_from_AC_ATR_72_REV05.pdf",
        xAw, yAw, zAw, iw,
        ComponentEnum.WING
    );

    theWing.calculateGeometry();
    theWing.getGeometry().calculateAll();

    // -----
    // Center of Gravity
    // -----

    double xCgLocal= 1.5; // meter
    double yCgLocal= 0;
    double zCgLocal= 0;

    CenterOfGravity cg = new CenterOfGravity(
        Amount.valueOf(xCgLocal, SI.METER), // coordinates in LRF
        Amount.valueOf(yCgLocal, SI.METER),
        Amount.valueOf(zCgLocal, SI.METER),
        Amount.valueOf(xAw, SI.METER), // origin of LRF in BRF
        Amount.valueOf(yAw, SI.METER),
        Amount.valueOf(zAw, SI.METER),
        Amount.valueOf(0.0, SI.METER), // origin of BRF
        Amount.valueOf(0.0, SI.METER),
        Amount.valueOf(0.0, SI.METER)
    );

    cg.calculateCGinBRF();
    theWing.set_cg(cg);
    theWing.set_aspectRatio(6.0);

    // Default operating conditions
    OperatingConditions theOperatingConditions = new OperatingConditions();
    theOperatingConditions.set_alphaCurrent(Amount.valueOf(2.0, NonSI.DEGREE_ANGLE)
```

```

// -----
// Define an LSAerodynamicsManager Object
// -----

LSAerodynamicsManager theLSSimulation = new LSAerodynamicsManager (
    theOperatingConditions,
    theWing
);

// -----
// Setup database(s)
// -----

theLSSimulation.setDatabaseReaders(
    new Pair(DatabaseReaderEnum.AERODYNAMIC,
        "Aerodynamic_Database_Ultimate.h5"),
    new Pair(DatabaseReaderEnum.HIGHLIFT, "HighLiftDatabase.h5")
);

// -----
// Assign Airfoil(s) ...
// -----

// Define airfoilRoot...

// -----
// Set Airfoil(s)
// -----

List<MyAirfoil> myAirfoilList = new ArrayList<MyAirfoil>();
myAirfoilList.add(0, airfoilRoot);
myAirfoilList.add(1, airfoilKink);
myAirfoilList.add(2, airfoilTip);
theWing.set_theAirfoilsList(myAirfoilList);
theWing.updateAirfoilsGeometry();
theLSSimulation.initializeDependentData();

}

```

4.4 Database in JPAD

In JPAD it is possible to consult external databases in .h5 format. **HDF 5** (Hierarchical Data Format Release 5) is a data file format designed by the *National Center for Supercomputing Applications* (NCSA) to assist users in the storage and manipulation of scientific data across different operating systems and machines.

To obtain the useful data in JPAD interpolating functions are used. These functions can be of one, two or three dimensions and read data from graphics that have been digitized previously. Starting from these digitalizations, databases in .h5 format are built. Reading data from databases is entrusted to methods of classes in the `database` package.

In order to read these databases, and obtain the useful data, it is necessary to define an object of the database reading class and associate it with the object of analysis.

This is a crucial step to read correctly the external data. In fact JPAD allows to work with an aircraft object or only with an isolated lifting surface object. Aircraft is usually composed of a fuselage, lifting surfaces, nacelle and power plant. Furthermore, Aircraft and Wing are associated with classes of calculation like `LSAerodynamicManager` or `ACAnalysisManager`. So it is necessary that these databases are also visible from these classes.

So because both in aircraft and in wing there is a lifting surface object, databases relative to wing are associated to `LSAerodynamicManager`.

4.4.1 Setup database

Here the database path it's created and associated to object that interpolates the required data from the .h5 file using a MyInterpolatingFunction object. After this it's possible to access the double value of the interpolating function using the standaloneutils method called value.

Now the procedure to assign the database is different if is used an Aircraft object or a Wing object.

4.4.2 Assign database using an Aircraft object

In order to assign correctly the database and associate it to all analysis management is necessary to practise the following order.

1. Define an Aircraft Object.

This command associates to Aircraft an object that defines the aerodynamic. From the wing it is possible to obtain the Wing, that is a LiftingSurface object.

2. Define an ACAnalysisManager object.

All the aircraft computations are managed by this class.

3. Define an LSAerodynamicManager object.

All the lifting surfaces computations are managed by this class.

4. Associate database to LSAerodynamicManager.

5. Eventually do analysis.

4.4.3 Assign database using a Wing object

Using a Wing object it isn't necessary to define a manager for Aircraft aerodynamic analysis. So the step to follow are the same of aircraft starting from the third.

1. Define a Wing Object.

2. Define an LSAerodynamicManager object.

3. Associate database to LSAerodynamicManager.

The definition of an isolated Wing is explained in the relative section.

Listing 4.3 Assign database using an Aircraft object

```
// -----
// Setup database(s)
// -----
theLSAnalysis.setDatabaseReaders(
    new Pair(DatabaseReaderEnum.AERODYNAMIC,
        "Aerodynamic_Database_Ultimate.h5"),
    new Pair(DatabaseReaderEnum.HIGHLIFT,
        "HighLiftDatabase.h5")
);
```

The databases are assigned to LSAerodynamic using a method of this class. This method accept as input a variable number of Pair objects. Using Pair objects it is possible to assign, for each database, both name and type.

Listing 4.4 setDatabaseReaders method

```
public void setDatabaseReaders(Pair... args) {
    String databaseFolderPath = MyConfiguration.getDir(FoldersEnum.DATABASE_DIR);

    for (Pair a : args) {
        DatabaseReaderEnum key = (DatabaseReaderEnum)a.getKey();
        String databaseFileName = (String)a.getValue();

        switch (key) {
            case AERODYNAMIC:
                _aerodynamicDatabaseReader =
                    new AerodynamicDatabaseReader(
                        databaseFolderPath,
                        databaseFileName);
                listDatabaseReaders.add(_aerodynamicDatabaseReader);
                break;

            case HIGHLIFT:
                _highLiftDatabaseReader =
                    new HighLiftDatabaseReader(
                        databaseFolderPath,
                        databaseFileName);
                listDatabaseReaders.add(_highLiftDatabaseReader);
                break;
        }
    }
}
```

4.4.4 User's guide

In order to execute some analysis in JPAD it is necessary, first of all, to define an analysis object in the Test class. The method `createDefaultAircraft` creates a new aircraft and the object that composes it. This method also populates the data of aircraft with default value corresponding to ATR-72 or Boieng 747_100B. Moreover the method `createDefaultAircraft` calls another method in Aircraft class: `initialize` that initializes the objects of the classes that perform calculations.

The purpose of this structure is to have only a way to assign the databases at an aircraft. Inasmuch as the wing is always present, the chosen strategy is to assign the database to the aerodynamic manager of the wing.

In order to bring to use the database also for the aircraft calculation, it is assigned at the aerodynamic manager of the aircraft in the method called `doAnalysis`.

At the same time `LSAerodynamicManager` sets itself as aerodynamic in the wing object. So it is possible to call the database using equally the following codes:

- `theWingObject.getAerodynamics.get_Database;`
- `theAircraftObject.get_theAerodynamic.get_Database;`
- `theLSManagerObject.get_Database;`
- `theACManagerObject.get_Database;`

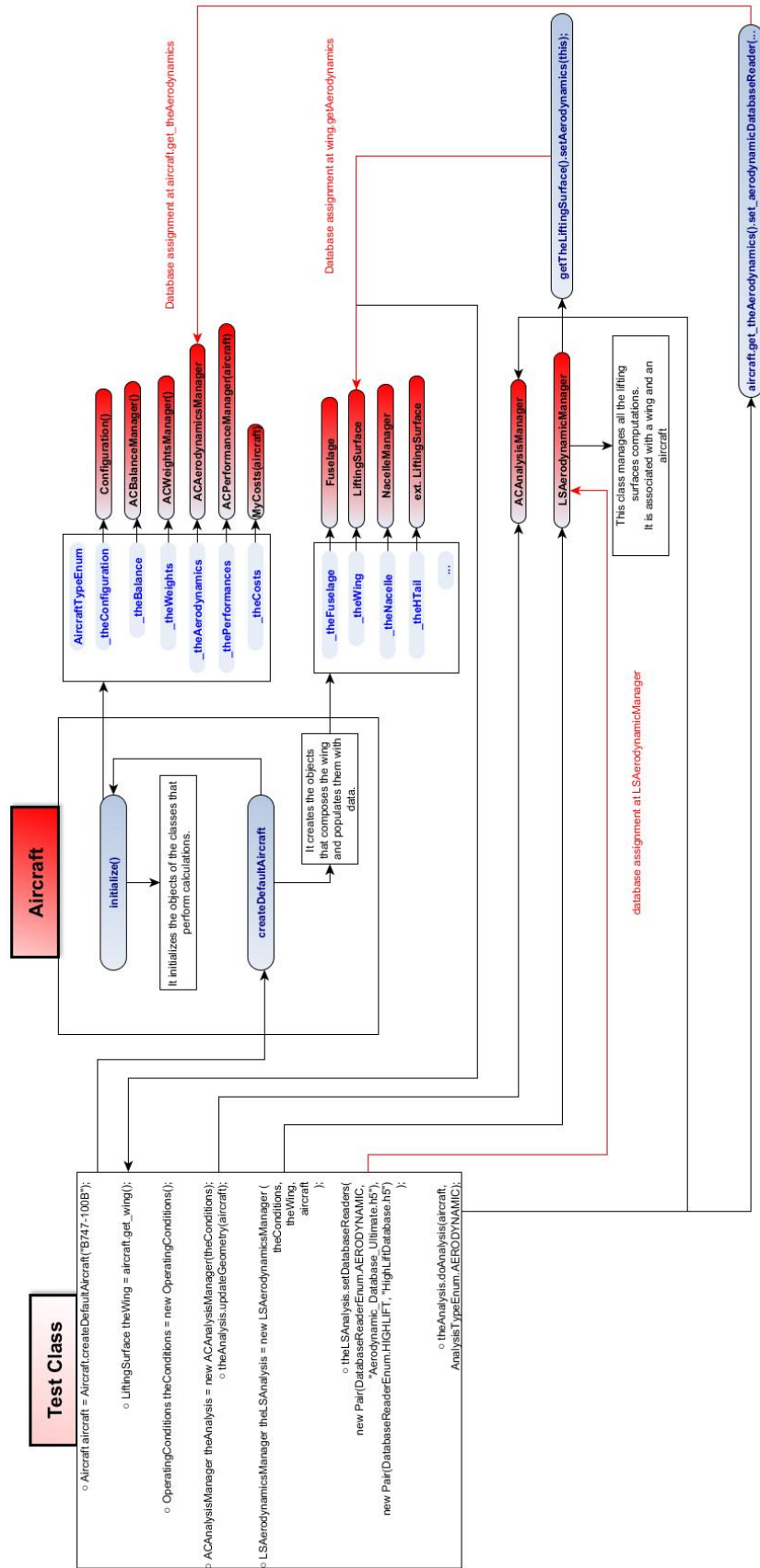


Figure 4.6: Flow chart of database assignment.

Part III

Functionality Overview

Chapter 5

Work Object Data

*Citazione
citazione
– Autore*

All the following analysis will be carried out using a default aircraft. This choice is made in order to avoid the collection and validation data phase for each analysis and make focus on the results. As mentioned, there are two default aircraft in the code: ATR-72 and Boeing 747_100B whose data are shown in the table below.

All the analysis that follow, refer to the data presented in this chapter and those derived from them .

Chapter 6

Wing Lift Characteristics

*If the facts don't fit the theory,
change the facts.*
– Albert Einstein

Any body in motion in a fluid presents a result of force acting on it, which can be decomposed in two components:

- A **Lift** acting normal to the Velocity direction and is positive upward.
- A **Drag** acting in the opposite direction to the airspeed vector.

The lifting surfaces of an airplane are designed to generate lift exceeding their drag, in order to obtain a positive efficiency.

In this chapter it will be explained how it's possible to evaluate the complete lift coefficient curve of a wing, both in its linear trait and non linear.

The lift coefficient is a dimensionless number used to model all of the complex dependencies of shape, inclination, and some flow conditions on lift. The lift coefficient also contains the effects of air viscosity and compressibility that are molded respectively with the Reynolds and Mach number.

6.1 Theoretical background

In order to achieve the complete curve of coefficient list it's necessary to obtain the following parameters:

1. Zero-Lift Angle
2. Lift Coefficient slope
3. End of Linearity Angle
4. Maximum Lift Coefficient
5. Stall Angle of attack

Following it will be explain the theory behind how these contributions have been made.

6.1.1 Zero-Lift Angle and Lift Coefficient Slope

In order to evaluate the linear trait of the wing lift curve, it's been used the Nasa-Blackwell method.

The **Nasa-Blackwell** is a numerical method for calculating the subsonic load distribution for arbitrary lifting surface arrangements at a fixed angle of attack. The method is suitable for swept wings, non-planar wings, wing with pylons and/or end-plates; it can be also used to study the aerodynamic interaction of the wing and the horizontal tail. The method has been implemented because its results, as shown in the report, were in good agreement with the experimental results. The lifting surfaces are divided in several rectangular horse-shoe vortices along the span; one horseshoe vortex along the chord is used, that is, the midpoints of the vortices are placed only at points along the quarter-chord lines. An equal number of control points are located along the three-quarter-chord lines. The velocity from the total vortex system is equated to the component of free-stream velocity normal to the lifting surface chord at each control point. Application of this tangent-flow boundary condition for a symmetrical loading provides a set of N simultaneous equations in the N unknown circulation strengths. Solution of this set of equations provides the loading distributions over the lifting surfaces. Mach number effect is introduced through a Prandtl-Glauert correction. Further details can be found in [20].

In this way it's calculated the Zero Lift angle using the integral of the load distribution and the linear trait slope starting from the value of CL at $\alpha = 0^\circ$ and $\alpha = 2^\circ$.

$$CL_\alpha = \frac{CL|_2 - CL|_0}{\Delta\alpha} \quad (6.1)$$

In JPAD it is possible also evaluating these two contributes using different methods. For the evaluation of the α_{0L} it's possible to use a method of the class `CalcAlpha0L`, a nested class in `LSAerodynamicManager`. Using these method, the zero-lift angle is calculated with the following formula, where ϵ_T is the twist angle:

$$\alpha_{0L} = \frac{1}{S} \int_{-\frac{b}{2}}^{\frac{b}{2}} c(y)[\alpha_0(y) - \epsilon_T(y)] dy \quad (6.2)$$

This formula is applied to the exposed wing. When a default aircraft is defined, during the creation of components, is calculated the exposed wing. This is the wing outside of the fuselage. It starts at semi-diameter of fuselage and its root airfoil is the airfoil of wing at this station calculated by the method `calculateIntermediateAirfoil`.

In order to evaluate the lift coefficient linear slope it's possible to use different method belonging to `CalcCLAlpha` class. The first one use the Polhamus formula which is valid for arbitrary aspect ratios and sweep angles in subsonic flow:

$$CL_\alpha = \frac{2\pi AR}{\left\{ 2 + \sqrt{\frac{AR^2\beta^2}{k^2} \left(1 + \frac{\tan^2(\Lambda_{\frac{c}{2}})}{\beta^2} \right)} + 4 \right\}} \quad (6.3)$$

Thus CL_α is a function of wing aspect ratio, mid-chord sweep angle $\Lambda_{\frac{c}{2}}$, Mach number, and airfoil section (defined parallel to the free stream) lift curve slope. The factor K in the equation is the ratio of the experimental two-dimensional lift curve slope.

Alternately it's possible to use the Anderson formula for swept wing, compressible and

subsonic flow:

$$CL_\alpha = \frac{Cl_\alpha \cos \Lambda_{\frac{c}{2}}}{\sqrt{1 - M^2 \cos^2 \Lambda_{\frac{c}{2}} + \left[\frac{Cl_\alpha \cos \Lambda_{\frac{c}{2}}}{\pi R} \right]^2} + \frac{Cl_\alpha \cos \Lambda_{\frac{c}{2}}}{\pi R}} \quad (6.4)$$

6.1.2 End of Linearity angle of attack

The angle of end linearity is calculated using the characteristics of the mean airfoil of the wing. This is obtained through the influence area of the airfoils as shown in fig. 6.1.

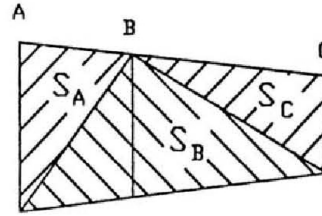


Figure 6.1: Influence area of the sections for finite wing.

Then is possible to calculate the influence coefficients.

$$K_i = \frac{2S_i}{S} \quad (6.5)$$

The mean parameters can be obtained from:

$$\bar{x} = x_1 K_1 + x_2 k_2 + x_3 k_3 \dots \quad (6.6)$$

In particular, for a wing defined by three airfoils, the end of linearity angle of attack is obtained from the following equation:

$$\alpha^* = \alpha_1^* K_1 + \alpha_2^* k_2 + \alpha_3^* k_3 \quad (6.7)$$

6.1.3 Maximum Lift Coefficient

In order to estimate the maximum lift coefficient for a clean wing it's been used the Nasa-Blackwell method.

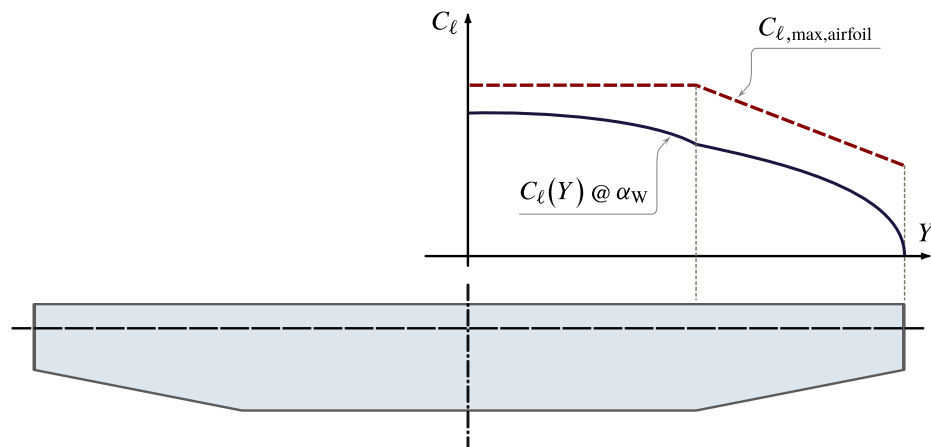


Figure 6.2: Determination of wing lift distribution and Cl distribution of airfoils.

The practiced procedure is the following:

1. For each value of an Alpha array the load distribution is calculated using the NasaBlack method. The distribution of Cl_{max} is known. fig. 6.3.
2. At $\alpha = \alpha_j$ the load distribution curve intersects for the first time the Cl_{max} curve of the airfoils. fig. 6.3.
3. For each $y > y_1$, along y axis (where y_1 is the station of first intersection) is evaluated the difference between CL_{wing} and Cl_{max} . fig. 6.4.
4. $\Delta\alpha$ is evaluated until the maximum difference between CL_{wing} and Cl_{max} is smaller than the required accuracy. Actually the accuracy is 0.0001.

The evauation of $\Delta\alpha$ is not simple.

After finding the first value of intersection between CL_{wing} and Cl_{max} a new α is evaluated. The first value used for the optimization is

$$\Delta\alpha = \alpha_j - \alpha_{j-1}$$

$$\alpha_{new} = \alpha_j - \frac{\Delta\alpha}{2}$$

$$\alpha_{old} = \alpha_j$$

For the following step if there isn't a point of intersectionat α_{new} the new value of α is, for the step $j + 1$:

$$\Delta\alpha = |\alpha_{j-1} - \alpha_j|$$

$$\alpha_{new} = \alpha_j + \frac{\Delta\alpha}{2}$$

$$\alpha_{old} = \alpha_j$$

Instead, if there is a point of intersectionat α_{new} the new value of α is, for the step $j + 1$:

$$\Delta\alpha = |\alpha_{j-1} - \alpha_j|$$

$$\alpha_{new} = \alpha_j - \frac{\Delta\alpha}{2}$$

$$\alpha_{old} = \alpha_j$$

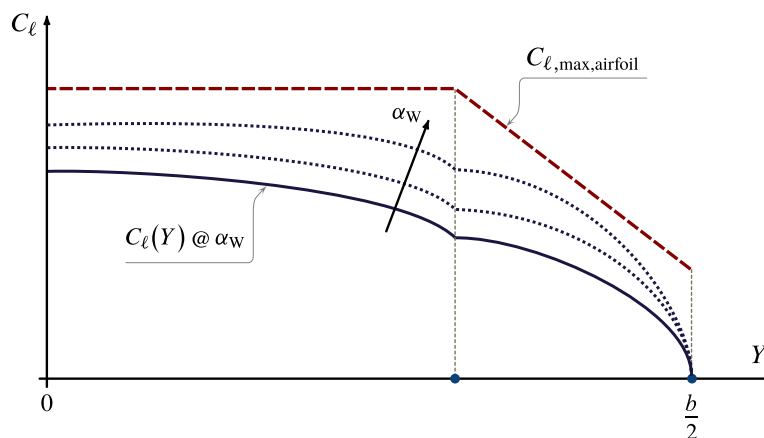


Figure 6.3: Determination of wing lift distribution and Cl distribution of airfoils.

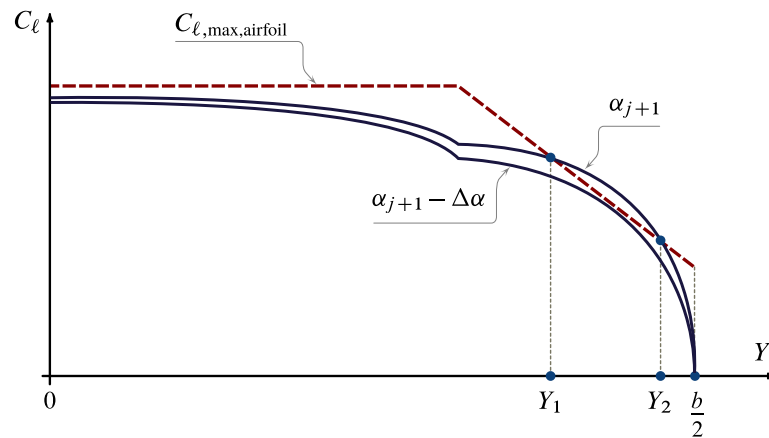
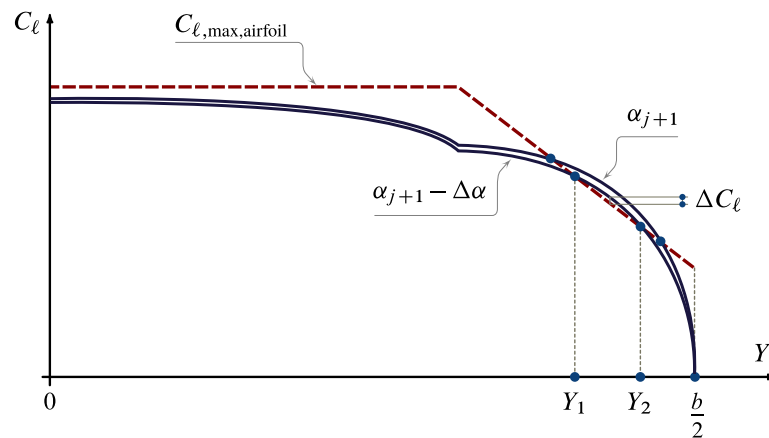
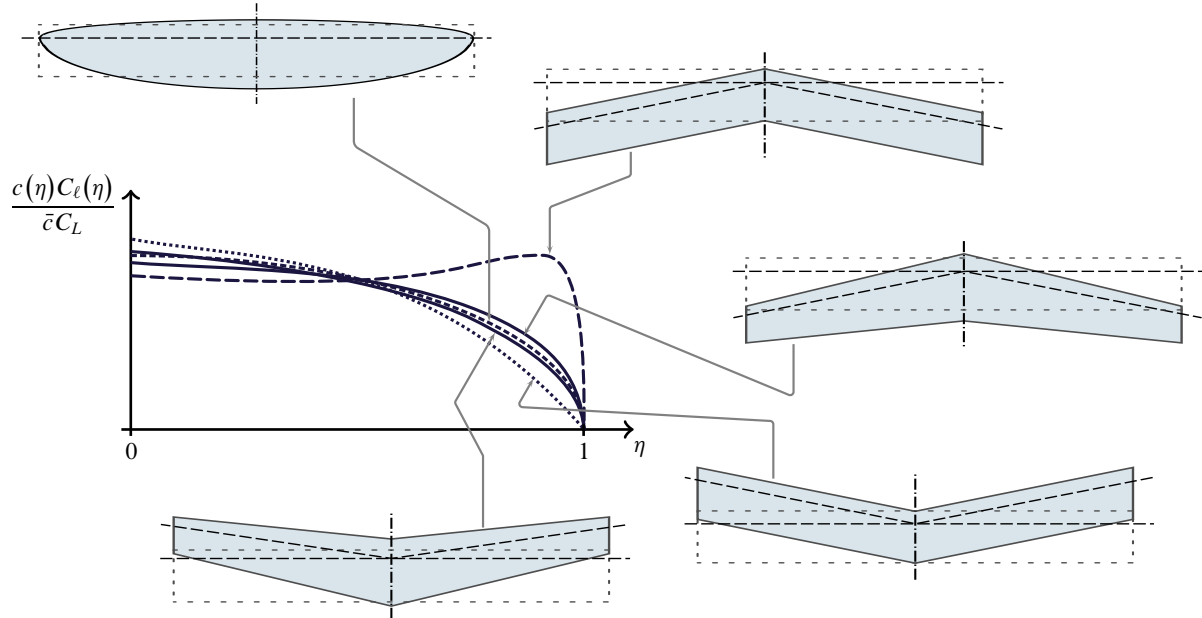
Figure 6.4: Intersection between CL_{wing} and $C_{l,max}$ curves.Figure 6.5: Determination of $\Delta\alpha$.

Figure 6.6: Wing Loading distribution.

6.1.4 Stall Angle of Attack

Nasa-Blackwell is an inviscid method for calculating the subsonic aerodynamic load distributions for arbitrary lifting-surface arrangements. This means that it doesn't see the non linear trait of the lift curve. So in correspondence of the value of $C_{L_{MAX}}$ calculated, the angle of attack obtained from the Nasa-Blackwell method is not correct because it is the maximum angle of attack that you would get if you reach the max C_L linearly.

Obtained the maximum C_L is therefore necessary to calculate the $\Delta\alpha$ from the following graph. So first it's evaluated the angle of attack at maximum lift coefficient through the linear trend of the lift line, then it's added to this angle the increment evaluated by the diagram in fig. 6.7. , this is valid strictly for wing with high taper ratio without twist, with unique airfoil type and Mach number included between 0.2 and 0.6.

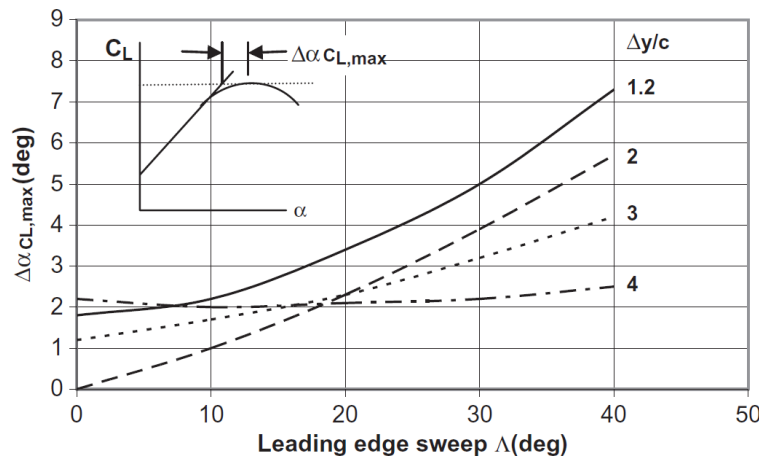


Figure 6.7: Diagram useful for evaluation of $\Delta\alpha$.

6.1.5 Construction of the curve

At this point all elements are available in order to draft the C_L vs α curve. The linear trait is evaluated using the equation of straight line.

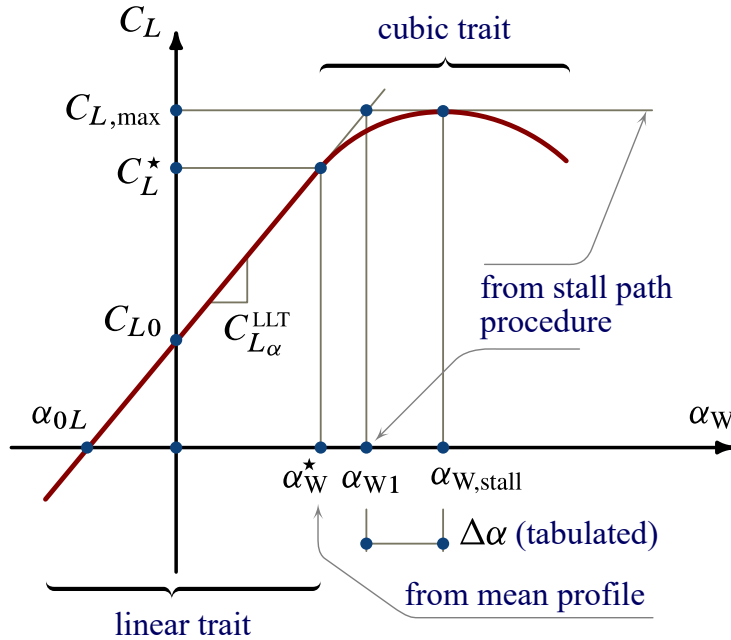
$$C_L = C_{L_\alpha} \alpha + C_{L_0} \quad (6.8)$$

In order to plot the non linear trait is used a cubic function. In fact in this zone we have four conditions:

- Pass to α^* , C_L^*
- The derivative in α^* , C_L^* is C_{L_α} for continuity
- Pass to α_{stall} , $C_{L_{MAX}}$
- The derivative in α_{stall} , $C_{L_{MAX}}$ is 0. Here there is the maximum of the curve.

So the system of equations is :

$$\begin{cases} C_L^* = a\alpha^{*3} + b\alpha^{*2} + c\alpha^* + d \\ C_{L_\alpha} = 3a\alpha^{*2} + 2b\alpha^* + c \\ C_{L_{MAX}} = a\alpha_{stall}^3 + b\alpha_{stall}^2 + c\alpha_{stall} + d \\ 0 = 3a\alpha_{stall}^2 + 2b\alpha_{stall} + c \end{cases} \quad (6.9)$$

Figure 6.8: Wing C_L vs α curve.

6.1.6 Mach number effects on Lift curve

The characteristics of airflow depend heavily from the Mach number. These changes in airflow have a significant effect on the airplane lift. For airplanes that operate entirely within the subsonic speed range, there are no significant effects of compressibility of the air on the airplane lift. For airplane that operate at high subsonic speeds in the transonic speed region, the airplane lift and drag curves will vary as the flight Mach number is increased due to the compressible nature of the air, so there is a family of lift curves one for each flight Mach number of interest.

The family of lift curves is characterized by an increase in the slope of the curve and decrease in maximum lift coefficient as the Mach number increased in the high subsonic region as shown in the fig. 6.9. The explanation of these Mach number effects on the lift curve has been derived from the theory of compressible flow, and confirmed by experimental data obtained in wind tunnels and from flight tests. It can be shown that, for an airplane at given angle of attack, the lift coefficient will increase with Mach number because the suction on the wing upper surface, and the pressures on the wing lower surface tend to grow with Mach number. [42]

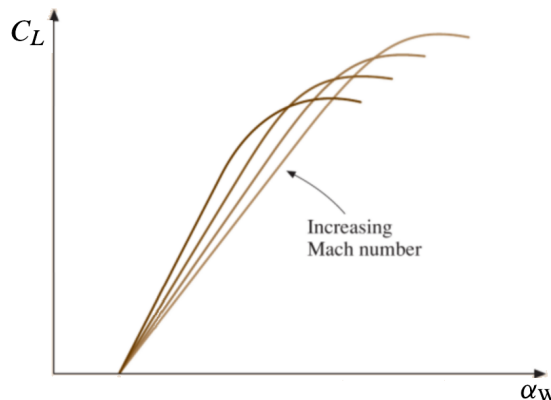


Figure 6.9: Mach number effects on Lift curve.

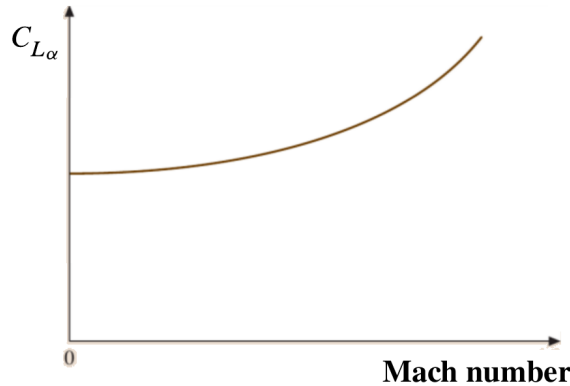


Figure 6.10: Mach number effects on Lift linear slope.

6.1.7 High Lift devices

The aircraft's performances at low speed are very important for their mission, in fact good high lift devices allow to land or take off on many airports, with their various runways.[25] To assure high lift in take-off and landing without varying weight and wing surface, it's varied the airfoil shape, for this reasons high-lift systems are used. High-lift systems are commonly defined as the devices that allow to increase the maximum lift coefficient of the aircraft and consequently to decrease the stalling speeds. A great variety of high lift devices exists, many of which are mechanically complex. The simplest systems change only the camber of the aerofoil. More complex concepts not only change camber but also extend the chord, opening up slots as they do so. [37]

High-lift devices can be classified in two main categories: trailing edge devices, or leading edge devices. TE devices are small aerofoil-like elements that are fitted at the trailing edge of the wing that are called flap, while at the LE as a slat.

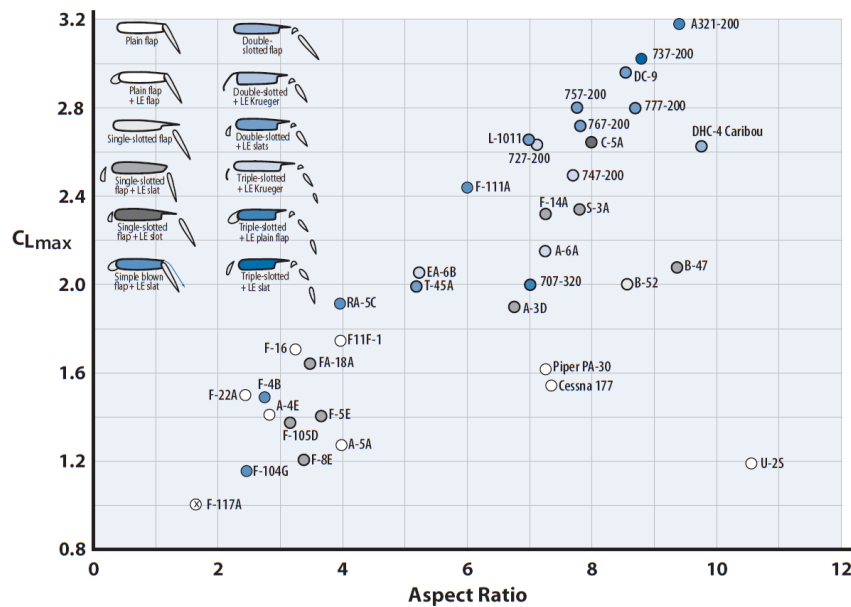


Figure 6.11: Different kind of High Lift devices and their effects.

In order to evaluate the new wing lift curve with flap and slat it's necessary to evaluate the contribution due to these devices starting from the clean C_L vs α curve. In particular these contribution on the lift curve are the following:

- ΔC_{L_0} flap
- $\Delta C_{L_{MAX}}$ flap
- CL_α flap
- $\Delta\alpha_{MAX}$ flap
- $\Delta C_{L_{MAX}}$ slat
- $\Delta\alpha_{MAX}$ slat

All of these parameters are calculated using formulas or graphs. For further details see [54]

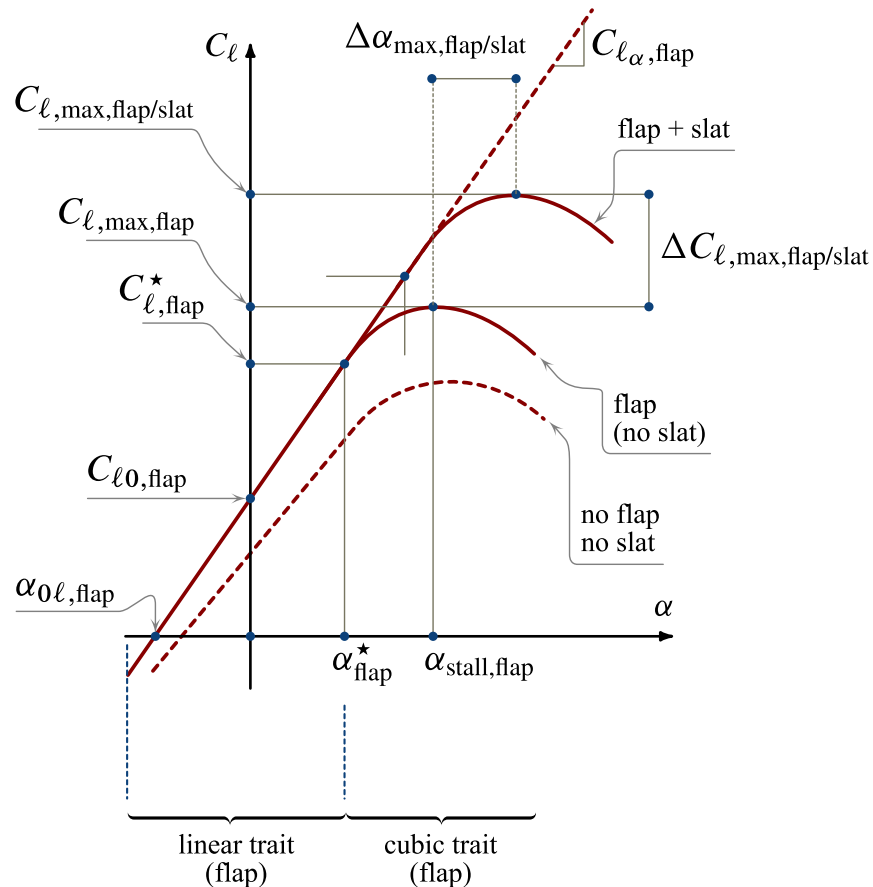


Figure 6.12: Wing C_L vs α curve for clean wing and with high lift devices.

6.2 Java Class Architecture

6.3 Case Study

Chapter 7

Wing Drag Characteristics

*It is not certain
that everything is uncertain*
– Blaise Pascal

As mentioned in the previous chapter, the drag is the force component acting in the opposite direction to the airspeed vector.

There isn't a single classification of the drag but, dependent on the purpose of the work, the drag may be broken down in different way. Following will be explained the two main classifications.

- The drag is subdivided using a causal breakdown. In this way the drag contributes are in accordance with the physical mechanism such as the viscosity of the flow.
- The drag is subdivided using a component breakdown. Every component of aircraft added an own drag contribute.

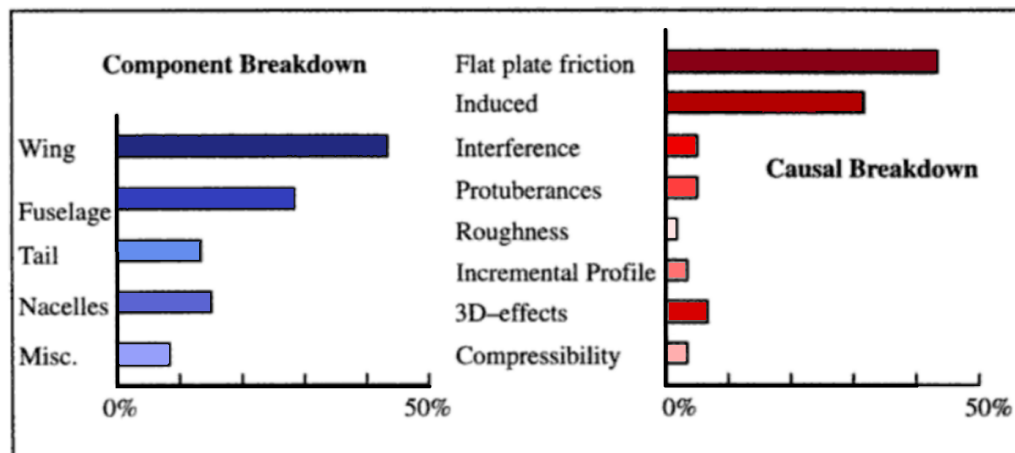


Figure 7.1: Drag breakdown for a business jet in cruise.

According to the causal breakdown it's possible to make a preliminary division considering normal and tangential stress. The tangential forces produce the **friction drag**. While it's possible to divide the drag due of the normal component in viscous, that generates **form drag**,

and inviscid. A further division can be made for the last one, in **induced drag** and **wave drag**.

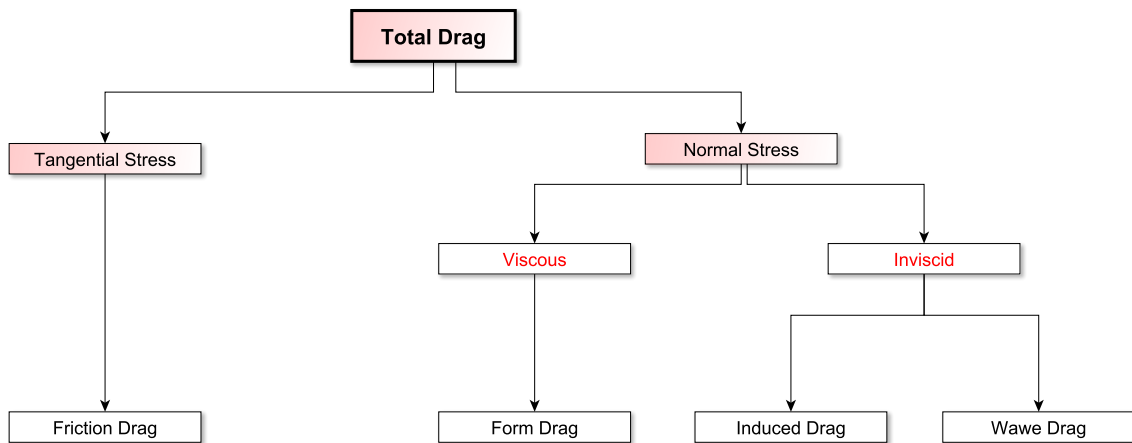


Figure 7.2: Causal breakdown of airplane drags.

Friction drag is caused by the air closest to the body's surface that is dragged along with it. Due to this interaction shearing stresses are born within the thin layer of air (boundary layer) adjacent to the skin. The magnitude of this drag depends on the kind of boundary layer what can be laminar or turbulent in dependence on the Raynolds number. Usually it's accustomed to assume, at the flight speed and altitudes at which aircraft fly, a fully turbulent flow over the entire airplane. In this way a conservative result is obtained.

Form drag is caused by the air that is flowing over the body. The separation of air creates turbulence and results in pockets of low and high pressure that leave a wake behind the airplane. The departure of the boundary layer alters the pressure field from its inviscid distribution resulting in an additional drag component. The general size and shape of the body are the most important factors in form drag; bodies with a larger presented cross-section will have a higher drag than thinner bodies.

Induced drag is the drag due to lift. It is the drag created by the vortices at the tip of an aircraft's wing. The high pressure underneath the wing causes the airflow at the tips of the wings to curl around from bottom to top in a circular motion. So it's depend on the spanwise distribution of lift.

Wave drag is a component of the drag due to the presence of shock waves. Wave drag is independent of viscous effects, and tends to present itself as a sudden and dramatic increase in drag as the vehicle increases speed.

In this work the drag will be classified using a component breakdown. In this way it's possible to evaluate separately the wing drag and tail drag, considering the aerodynamic centers of these lifting surfaces as application point.

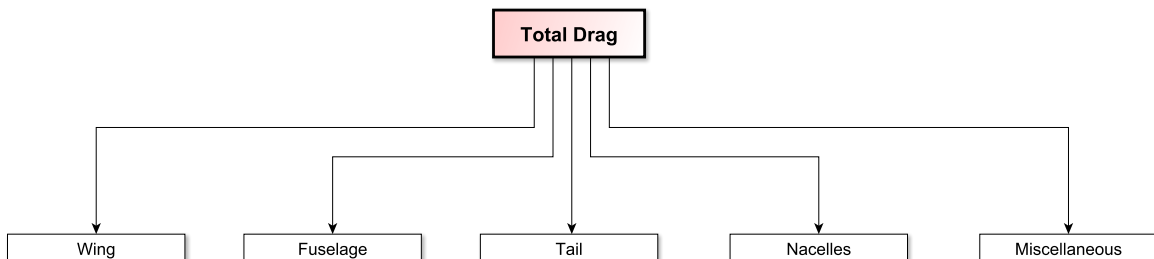


Figure 7.3: Components breakdown of airplane drags.

7.1 Theoretical background

In this thesis the drag coefficient of an isolated lifting surface is calculated starting from the load distribution and considering the parabolic approximation for the drag polar. The implemented process is the following:

1. First of all the load distribution at a given angle of attack has been calculated
2. Fifty points along the semispan are defined
3. For each point, an intermediate profile is calculated
4. To each profile correspond the lift coefficient at that station
5. Starting from the CL, using a parabolic approximation for the drag polar, the CD is calculated with the following equation

$$CD = CD_{min} + (CL - CL_{CD_{min}})^2 + k \quad (7.1)$$

6. Known the drag distribution it is possible to calculate the drag coefficient of the lifting surface integrating

In the tool it is possible to choose the method used to calculate the load distribution. In particular it's possible to use Shrenk or Nasa-Blackwell method.

Schrenk Method is based on an elliptical lifting coefficient distribution span wise hypothesis on the wing. This method also assumes that the pressure distribution is proportional to the wing area.

The **Nasa-Blackwell**, as mentioned, is a numerical method for calculating the subsonic load distribution for arbitrary lifting surface arrangements at a fixed angle of attack. 6

7.2 Java Class Architecture

In order to give more flexibility to the code, the calculation of drag coefficient is made from three different class summarized in the following table.

integralFromCdAirfoil	This method calculates the drag coefficient of the lifting surface using an integral and calling other method that fills the needed field. This is in the nested class <code>CalcCDAtAlpha</code>
nasaBlackwell	This method calculates drag distribution starting from the load distribution calculated with Nasa-Blackwell method and using a parabolic approximation for the drag polar. This is in the nested class <code>CalcCdDistribution</code>
nasaBlackwell	This method calculates the drag coefficient of an airfoil having the lift coefficient and using a parabolic approximation.

Table 7.1: Methods for drag coefficient calculator of a lifting surface.

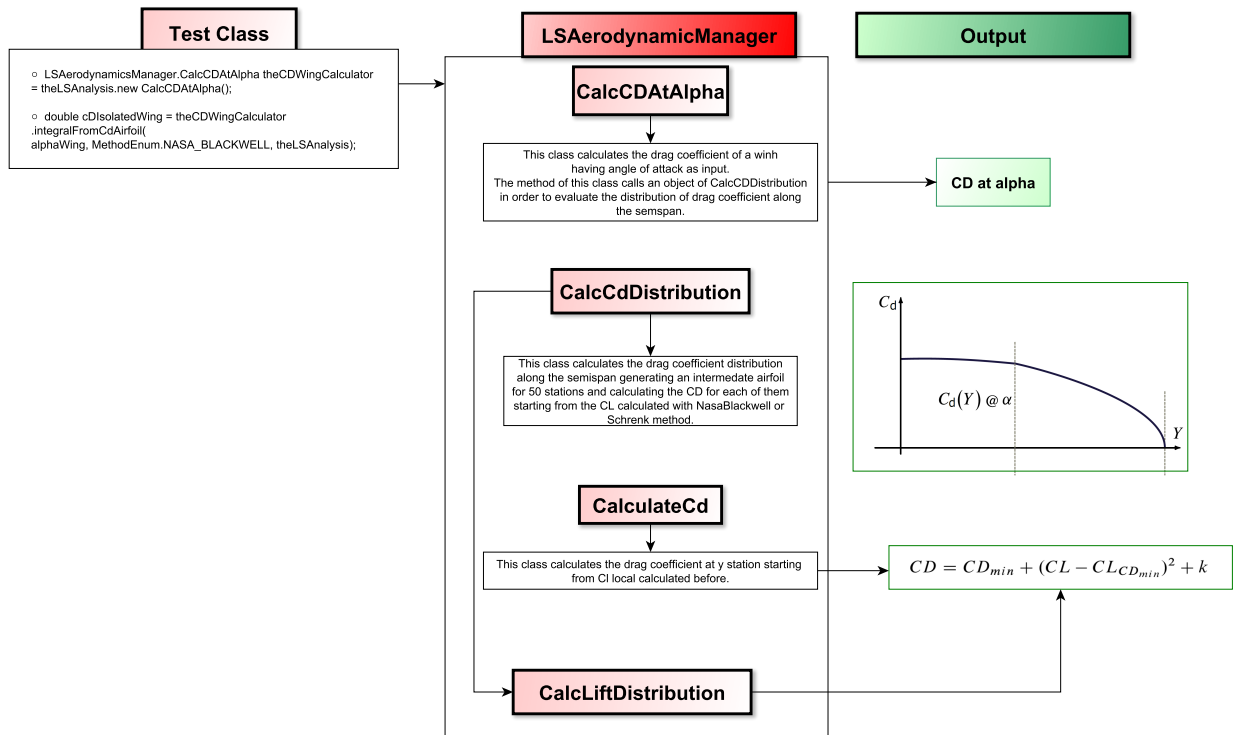


Figure 7.4: Flow chart of drag estimation classes.

7.3 Case Study

After initializing the Test class and defining the work object, it is possible to define an object of the class CalcCDAtAlpha that calculates the drag coefficient of a wing at a given angle of attack. This method accepts as input three parameters: the angle of attack of the wing, the method used in order to calculate of lift distribution and an object of the lifting surface aerodynamic manager.

The it is possible to plot the curves of drag coefficient versus α_w or lift coefficient that is the drag polar of the wing.

Listing 7.1 Use of Drag Calculator class

```

// -----
// DRAG CHARACTERISTICS
// -----
System.out.println("\n\n-----");
System.out.println("\n\u2014DRAG_CHARACTERISTICS\u2014");
System.out.println("\n-----");

LSAerodynamicsManager.CalcCDAtAlpha theCDWingCalculator = theLSAnalysis
        .new CalcCDAtAlpha();
double cDIsoletedWing = theCDWingCalculator.integralFromCdAirfoil(
        alphaWing, MethodEnum.NASA_BLACKWELL, theLSAnalysis);
System.out.println("CD_of_Wing_at_alpha_body="+(deg)
        + alphaBody.to(NONSI.DEGREE_ANGLE).getEstimatedValue()
        + "is "+ cDIsoletedWing);

System.out.println("....waiting_for_plotting");
theLSAnalysis.PlotCDvsAlphaCurve(subFolderPath);
System.out.println("\n\n\t\t\tDONE_PLOTTING_CD_vs_ALPHA_WING");
}

```

Following there are the summary diagrams of the results obtained for the ATR 72:

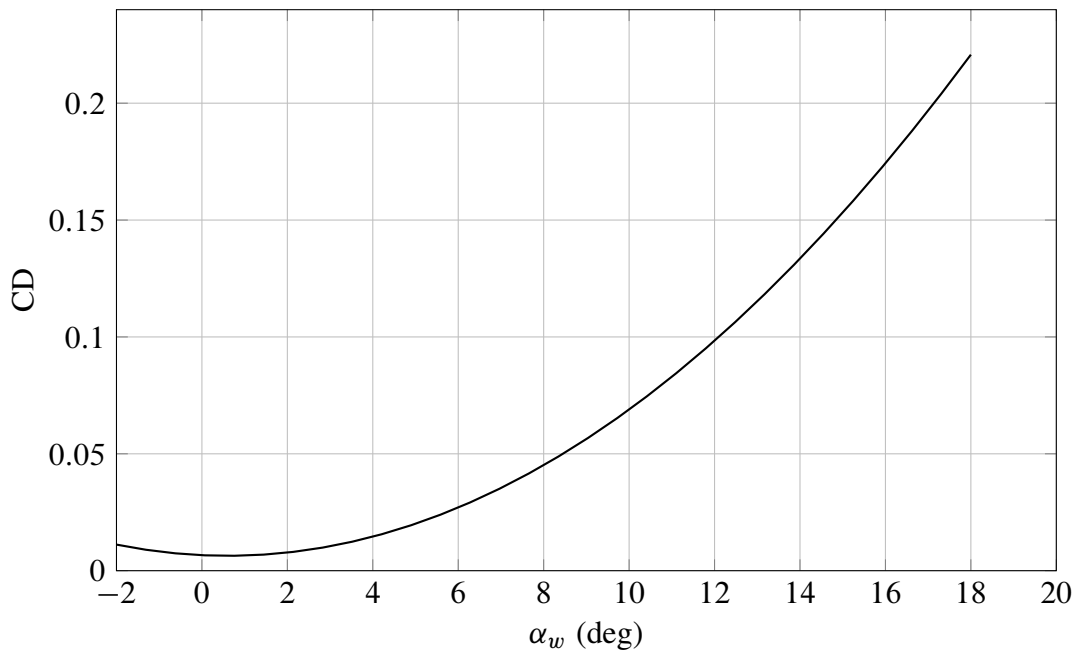


Figure 7.5: ATR 72 CD vs Alpha_w at Mach 0.43 and Altitude: 6000 m.

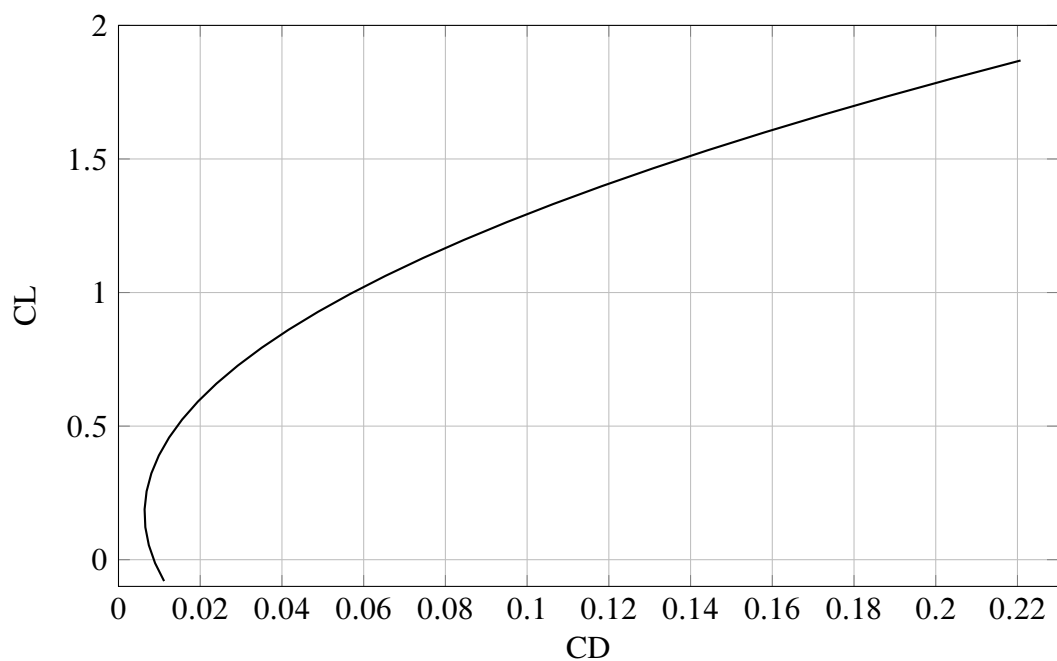


Figure 7.6: ATR 72 Parabolic Polar Drag at Mach 0.43 and Altitude: 6000 m.

Chapter 8

Downwash Estimation

*The important thing is not to stop questioning.
Curiosity has its own reason for existing.*
– Albert Einstein

In order to evaluate the characteristics of longitudinal stability of an aircraft it's necessary to assess the flow direction aft of the wing. The contribution of horizontal tail surface to the airplane equilibrium and stability, in fact, depends seriously on the flow direction. The purpose of this chapter is to introduce and evaluate the downwash gradient due from the wing's vortex system, considering a dependence of the downwash angle from the absolute angle of attack.

8.1 Theoretical background

Due to the finite extension of the wing the lift distribution in span is not uniform. For this reason the difference of pressure between upper and lower surfaces generates a movement of air around the wingtips. The tendency is for particles of air to move from the region of high pressure around the wing tip to the region of low pressure (from positive lift from the lower wing surface to the upper surface). This made the wing's vortex system that consisting of the bound vortex, located at the wing quarter chord and a vortex sheet which rolling up, at the wing tip, in two trailing vortex.[57] [71]

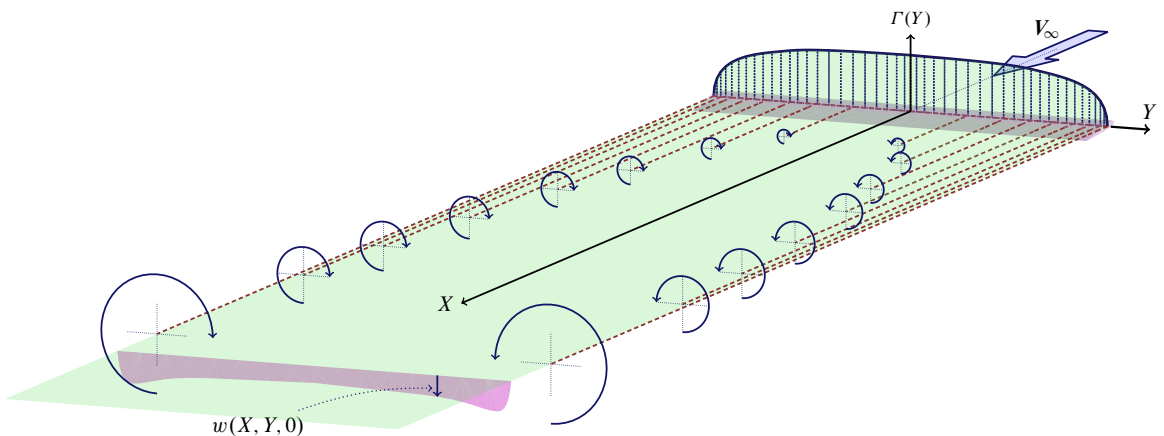


Figure 8.1: The wing vortex sheet.

The main effect of this vortex system is to deflect the airflow behind the wing downward relative to the direction of freestream flow. This angle of deviation is known as *Downwash Angle* ϵ . This phenomenon occurs for every lifting surface, but in subsonic flow a lifting surface also affects the flow forward of itself. In this region the vortex creates an itshape upwash, that is an upward flow deflection.

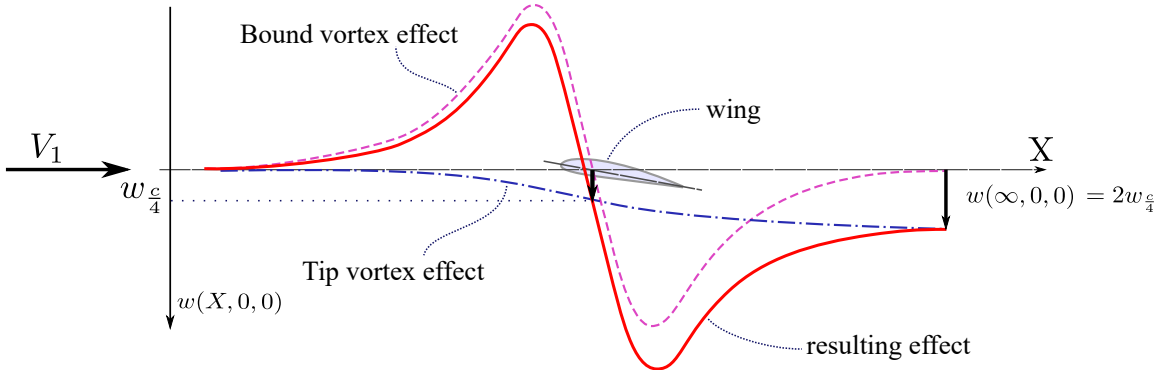


Figure 8.2: Upwash and Downwash in a finite wing.

As consequence of the downwash behind the wing, the local angle of attack on the horizontal tail is reduced by ϵ . In order to evaluate the flow direction behind the wing, an other important parameter is the change in downwash angle with angle of attack, that is the *Downwash Gradient* $\frac{d\epsilon}{d\alpha}$.

This parameter depends principally on the location of the horizontal tail with respect to the wing and the vortex plane. As first approximation this value could be considered constant in alpha, but more accurately it's possible to evaluate this dependence considering the reference variable for the calculation of the distances. Both if the vertical distance is considered as constant and it is considered variable with alpha, starting from the downwash gradient, the downwash angle is :

$$\epsilon = \frac{d\epsilon}{d\alpha_w} (\alpha_w - \alpha_{0w}) \quad (8.1)$$

In order to evaluate the downwash gradient it refers to fig. 8.3, where “ $r \frac{b}{2}$ ” is the distance between the aerodynamic center of wing and the aerodynamic center of the horizontal tail. This is a geometric an fixed distance. Conversely, in order to have a greater accuracy it's possible to consider the distance “ $m \frac{b}{2}$ ” variable with the angle of attack. Properly this is the distance between the horizontal tail and the vortex shed plane, but it's possible to approximate it with the distance between the horizontal tail and the wing root chord.[69]

Referring to the equation used in order to evaluate the downwash gradient is the following:

$$\frac{d\epsilon}{d\alpha} = \frac{K_{\epsilon A}}{K_{\epsilon A=0}} \left(\frac{r}{r^2 + m_{tv}^2} \frac{0.4876}{\sqrt{r^2 + 0.6319 + m_{tv}^2}} + \left[1 + \left(\frac{r^2}{r^2 + 0.7915 + 5.0734m_{tv}^2} \right)^{0.3113} \right] \left\{ 1 - \sqrt{\frac{m_{tv}^2}{1 + m_{tv}^2}} \right\} \right) \frac{C_{L\alpha_w}}{\pi AR} \quad (8.2)$$

Considering a variable downwash gradient the changing parameter is $m \frac{b}{2}$.

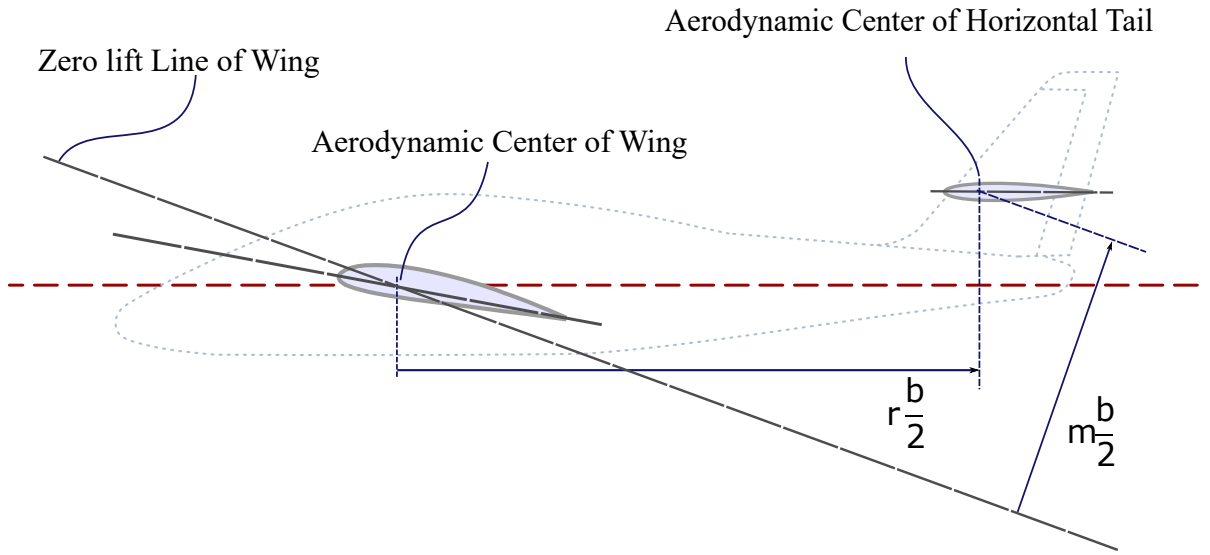


Figure 8.3: Dimensions for determination of Downwash Gradient, considering constant distances.

The two K_ϵ terms in the eq 8.3 accounting for the wing sweep angle effect are defined as follow (where Λ expressed in radians):

$$K_{\epsilon \Lambda} = \frac{0.1124 + 0.1265\Lambda + 0.1766\Lambda^2}{r^2} + \frac{0.1024}{r} + 2 \quad (8.3)$$

$$K_{\epsilon \Lambda=0} = \frac{0.1124}{r^2} + \frac{0.1024}{r} + 2 \quad (8.4)$$

These two terms are constant with α because it does not appear the variable parameter in them.

8.2 Java Class Architecture

In order to simplify the calculation of downwash, as mentioned, it's possible to assume the downwash gradient constant with the angle of attack. In this case the reference line to calculate the distance along z axis is the plane from the wing root chord or else the zero-lift line of the wing.

To obtain a more accurate analysis it's possible to consider the variation in alpha of the downwash gradient. So the reference line of wing it's not costant, but is the vortex sheet plane. The location of this plane depends from the value of downwash, but this location is itself necessary to evaluate the downwash. So it's necessary an iterative process in which the position of the vortex reference line at alpha is calculated from the value of downwash gradient at previous step.

In this process the reference angle of attack is the absolute angle α_a , that is the angle between the flow direction and the zero lift line of the wing. This choice is necessary because for $\alpha_a = 0$ it's possible to assume the downwash zero, but the downwash gradient is not null. In this way it's possible to assume the downwash value in the first step of the iteration and to continue for each step with the previous value as first attempt. In view of stability, however, the reference angle of attack is the α_B . There two angles they are related by the relation: $\alpha_B = \alpha_{0L} - i_w + \alpha_a$.

The relation between the angles is in the fig ??.

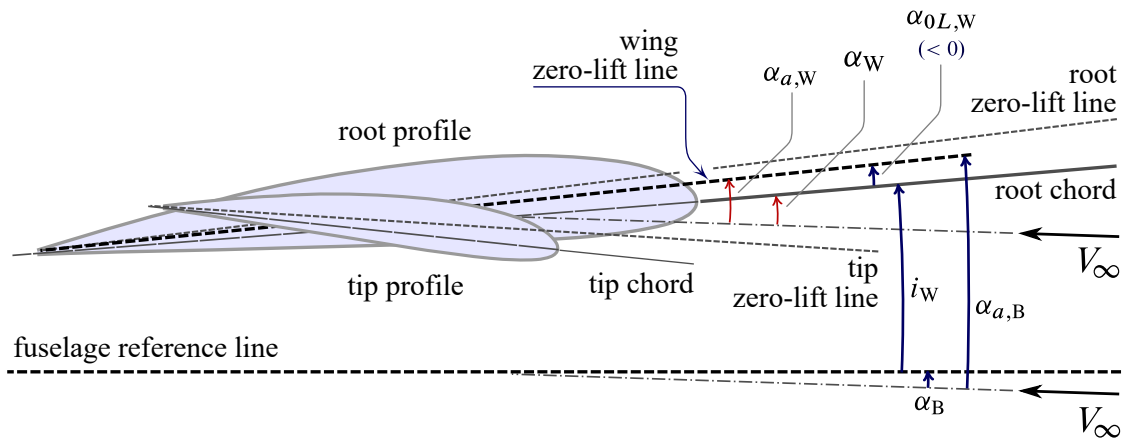


Figure 8.4: Definition of wing angles.

The downwash angle is calculated by a class named `DownwashCalculator`. The builder of this class defines and assings all the geometrical variables, necessary to implement the calculation. The `DownwashCalculator` class has seven methods and some overloads. The methods are explained in the table 8.1. The methods will be explained more in detail below.

<code>calculateDownwashGradientConstantDelft</code>	This method calculates the downwash gradient considering the vertical distance geometrical and constant
<code>calculateDownwashNonLinearDelft</code>	This method calculates the downwash considering a non constant downwash gradient.
<code>getDownwashAtAlphaBody</code>	This method returns the value of downwash angle, interpolating data filled before.
<code>calculateZDistanceZeroLift</code>	This method calculates the distance between the aerodynamic centre of horizontal tail and the zero lift line of the wing.
<code>Plot Methods ...</code>	Using these methods it's possible to plot the downwash angle, the downwash gradient and the distance in function of α_B

Table 8.1: Methods of `DownwashCalculator` class.

8.2.1 Constant Downwash Gradient

In order to evaluate the downwash angle case of constant downwash gradient it's necessary only to call the method `calculateDownwashGradientConstantDelft` using the distance from aerodynamic center of horizontal tail and the alpha zero lift line as input. It's possible to calculate this distance geometrically using the method `calculateZDistanceZeroLift` of the same class. The choice to calculate separately the distance and

the downwash gradient is made to reuse the method to calculate downwash gradient simply varying the input distance.

This method has the downwash gradient as output. To obtain the angle of downwash it simply need to moltiplicate the output value and the absolute angle of attack.

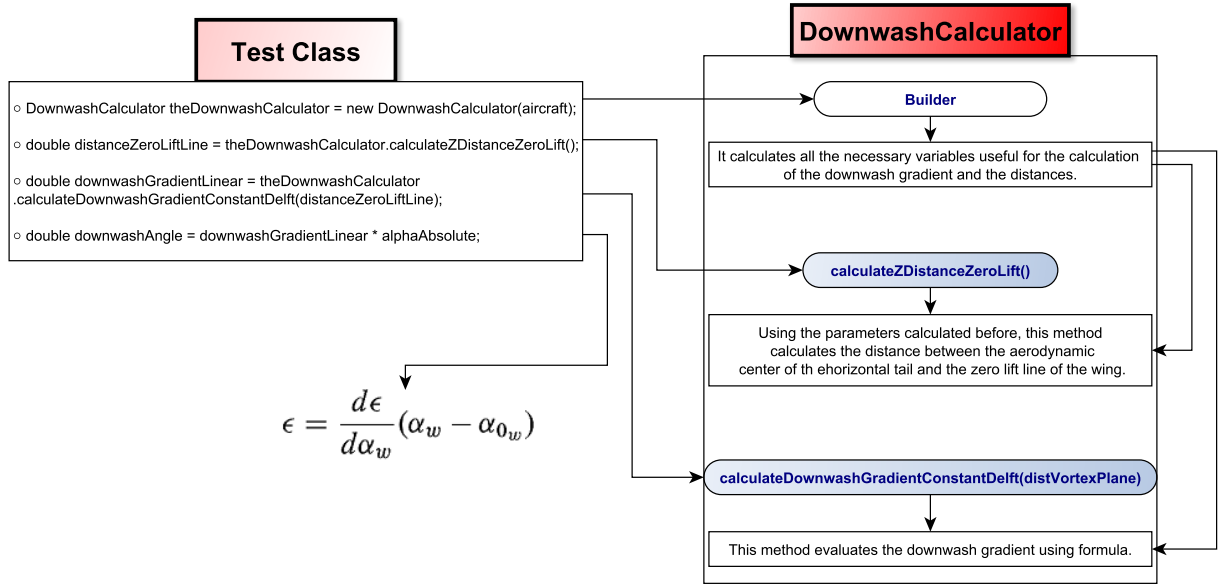


Figure 8.5: Flow chart of the calculation of linear downwash angle.

8.2.2 Variable Downwash Gradient

In order to evaluate the non-constant downwash gradient must use the method `calculateDownwashNonLinearDelft`. This method calculates the downwash gradient using Delft formula. The downwash gradient is considered variable in alpha absolute. The distance along x considered in the formula is geometric and fixed. Conversely the other distance is variable and it is considered as the distance between the horizontal tail the vortex shed plane. This method works through the following steps:

1. First of all this method creates an array of absolute angle of attack starting from $\alpha = 0^\circ$ to $\alpha = 20^\circ$ with a step of 0.25° .
2. The results array are initialized (α_a , α_B , $\frac{d\epsilon}{d\alpha}$, ϵ , $m\frac{b}{2}$).
3. For the first step the state is the following:
 - $\alpha_a = 0^\circ$
 - $\alpha_B = \alpha_{0L} - i_w$
 - $\frac{d\epsilon}{d\alpha}$ is the constant value
 - $m\frac{b}{2}$ distance is the same of the previous case and it is calculated using the method `calculateZDistanceZeroLift`.
 - $\epsilon = 0$
4. Starting from the second step the process is iterative. Starting from $\alpha_a = 0^\circ$ the absolute angle of attack increase of $\Delta\alpha$. For the step i:
 - $\alpha_a|_i = i \Delta\alpha$

- $\epsilon_{temp} = \frac{d\epsilon}{d\alpha}|_{i-1} * \alpha_a|_i$
- $m\frac{b}{2}|_{temp}$ is calculated considering the temporary value of downwash angle.
- $\frac{d\epsilon}{d\alpha}|_{temp}$ is calculated using the formula and the temporary value of distance.
- $\epsilon_i = \frac{d\epsilon}{d\alpha}_{temp} * \alpha_a|_i$
- $m\frac{b}{2}|_i$ is calculated considering the new value of downwash angle.
- $\frac{d\epsilon}{d\alpha}|_i$ is updated.
- $\alpha_B = \alpha_{0L} - i_w + \alpha_a$

In order to relieve the calculations, the evaluation of downwash angle and downwash gradient should be done only one time. To obtain the value of epsilon at alpha body it's possible to call the method `getDownwashAtAlphaBody` that interpolates the value of downwash angle and angle of attack which field must be filled before.

Step by step the value of $m\frac{b}{2}$ is calculated with the following geometrical construction:

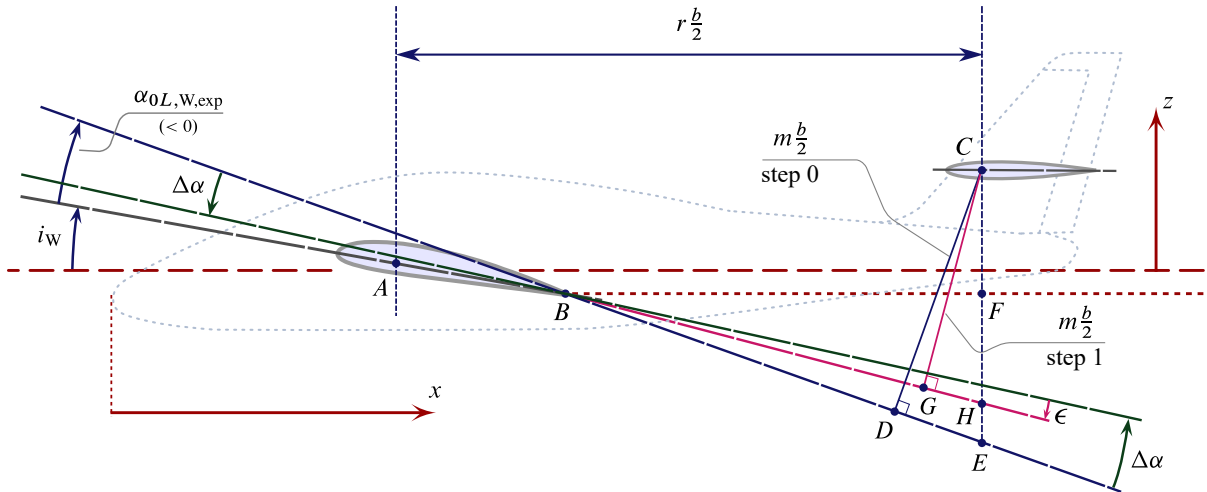


Figure 8.6: Arm definitions for downwash gradient evaluation.

Referring to the step 0, the distance $m\frac{b}{2}$ is the segment \overline{CD} . It's possible to calculate this distance geometrically as follows:

$$\overline{CD} = (\overline{CF} + \overline{FE}) * \cos(i_w - \alpha_{0L}) \quad (8.5)$$

\overline{CF} is the distance along Z between the aerodynamic center of horizontal tail and the trailing edge of root airfoil of the wing.

$$\overline{CF} = Z_{ac_H} - Z_{ac_W} \quad (8.6)$$

Is possible to calculate the distance \overline{FE} considering the triangle BFE . The side \overline{BF} is the distance along X axis between the aerodynamic center of horizontal tail and the trailing edge of root airfoil of the wing, while the angle between this side and the hypotenuse is $i_w - \alpha_{0L}$.

For each step the method is the same, but the difference is that the angle $i_w - \alpha_{0L}$ becomes $i_w - \alpha_{0L} - i \Delta\alpha + \epsilon$. In this way the distance that changes is \overline{FE}

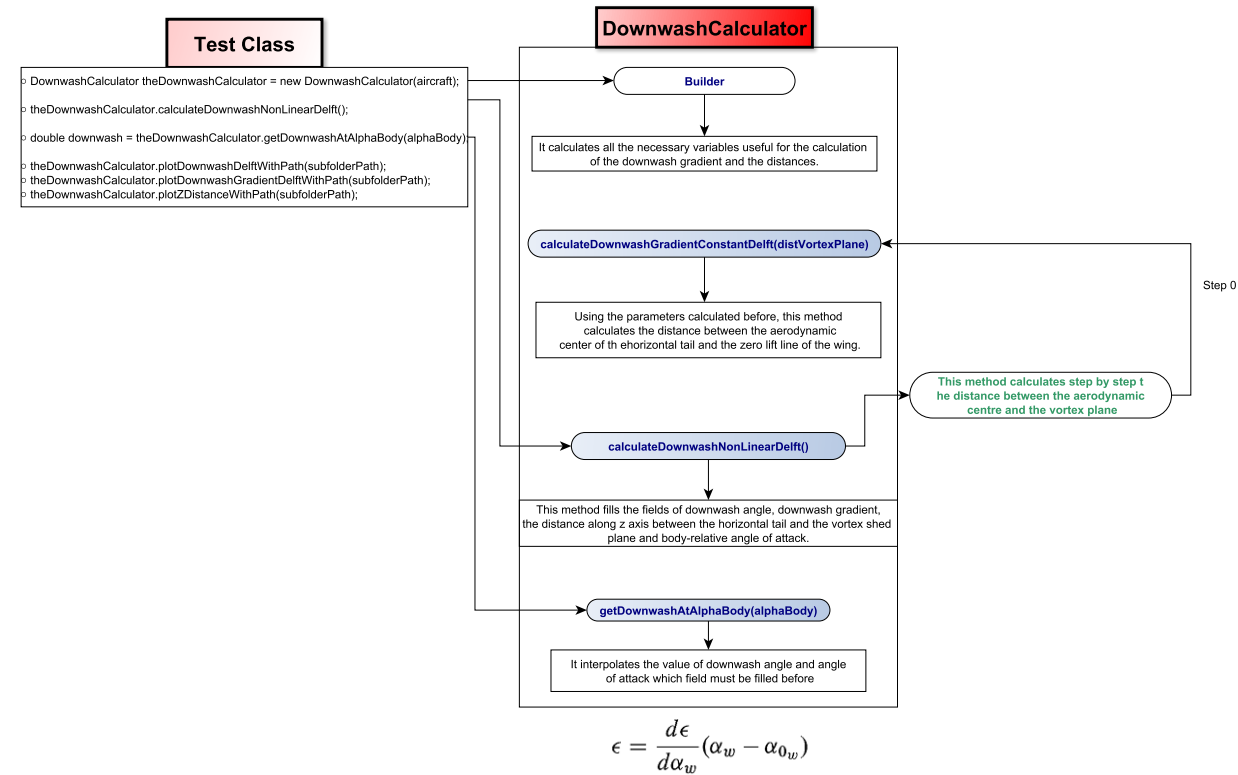


Figure 8.7: Flow chart of the calculation of non-linear downwash angle.

8.3 Case Study

In the following listing is reported the Test Class used in order to evaluate the variability of the downwash gradient with α_B . First of all the test class is initialized, after an Aircraft object is defined with the related analysis classes.

Listing 8.1 Downwash Test Class

```

// -----
// INITIALIZE TEST CLASS ...
// -----

// -----Downwash-----

System.out.println("\n-----Start_of_downwash_calculation-----\n" );
DownwashCalculator theDownwashCalculator = new DownwashCalculator(aircraft);
theDownwashCalculator.calculateDownwashNonLinearDelft();

theDownwashCalculator.plotDownwashDelftWithPath(subFolderPath);
theDownwashCalculator.plotDownwashGradientDelftWithPath(subFolderPath);
theDownwashCalculator.plotZDistanceWithPath(subFolderPath);
System.out.println("_DONE_PLOTTING_DOWNWASH_ANGLE_vs_ALPHA_BODY");

double downwash = theDownwashCalculator.getDownwashAtAlphaBody(alphaBody);
Amount<Angle> downwashAmountRadian = Amount
    .valueOf(Math.toRadians(downwash), SI.RADIAN);
System.out.println("At_alpha_" + alphaBody
    .to(NonSI.DEGREE_ANGLE)
    .getEstimatedValue() + "_(deg)_the_downwash_angle_is_(deg)_=" + downwash );

}

}

```

Below are the charts representing the results obtained by applying the method described in ATR 72.

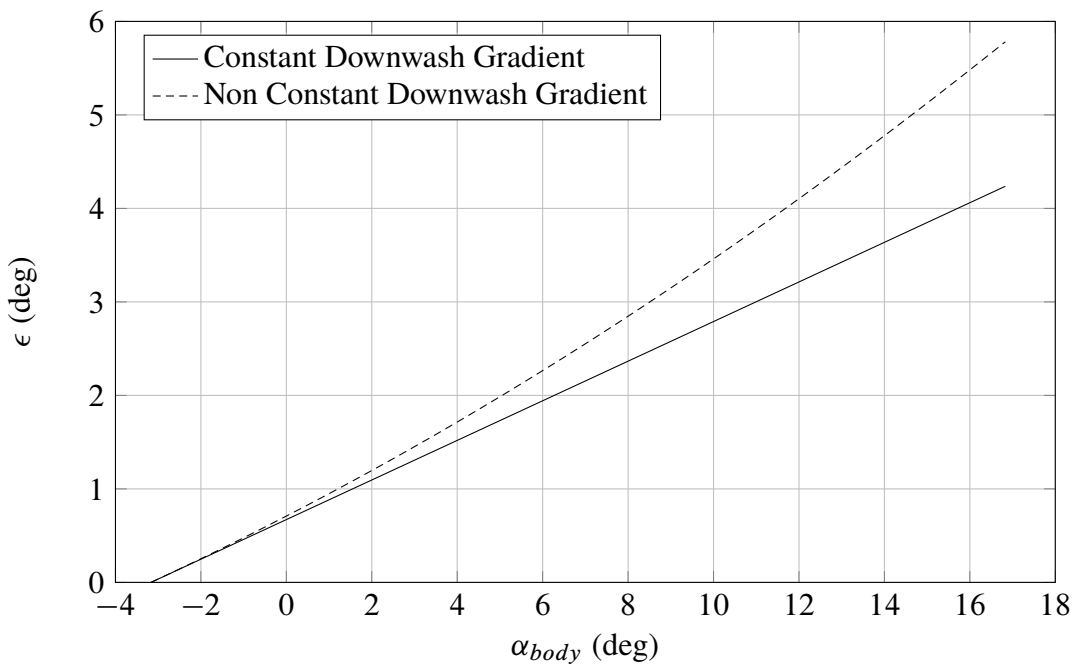


Figure 8.8: ATR 72 Downwash angle vs α_B .

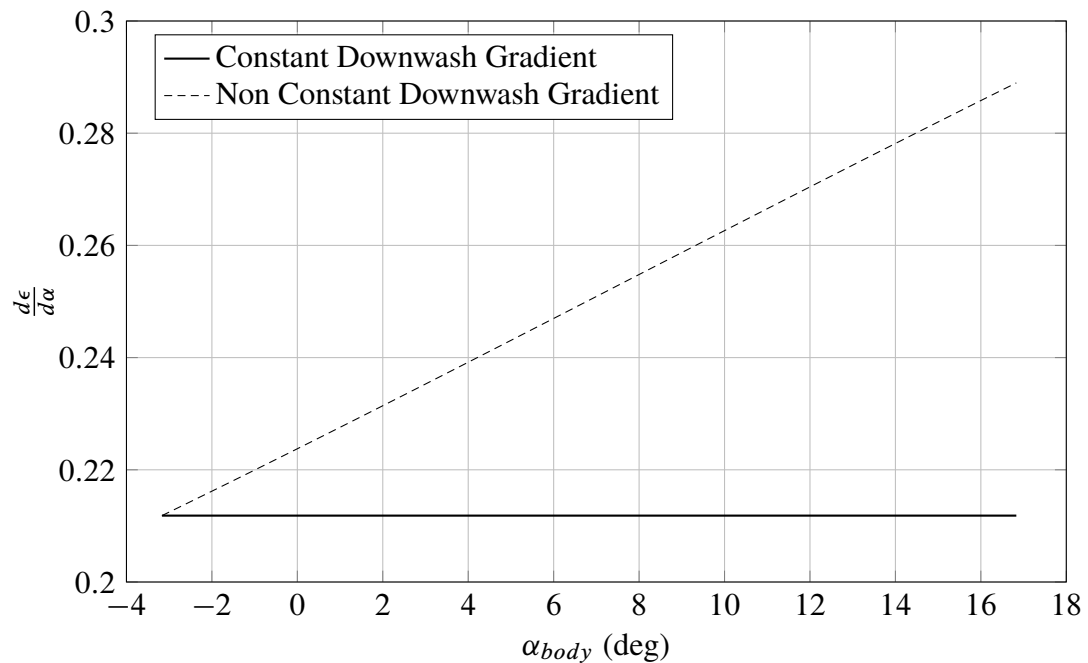


Figure 8.9: ATR 72 Downwash gradient vs α_B .

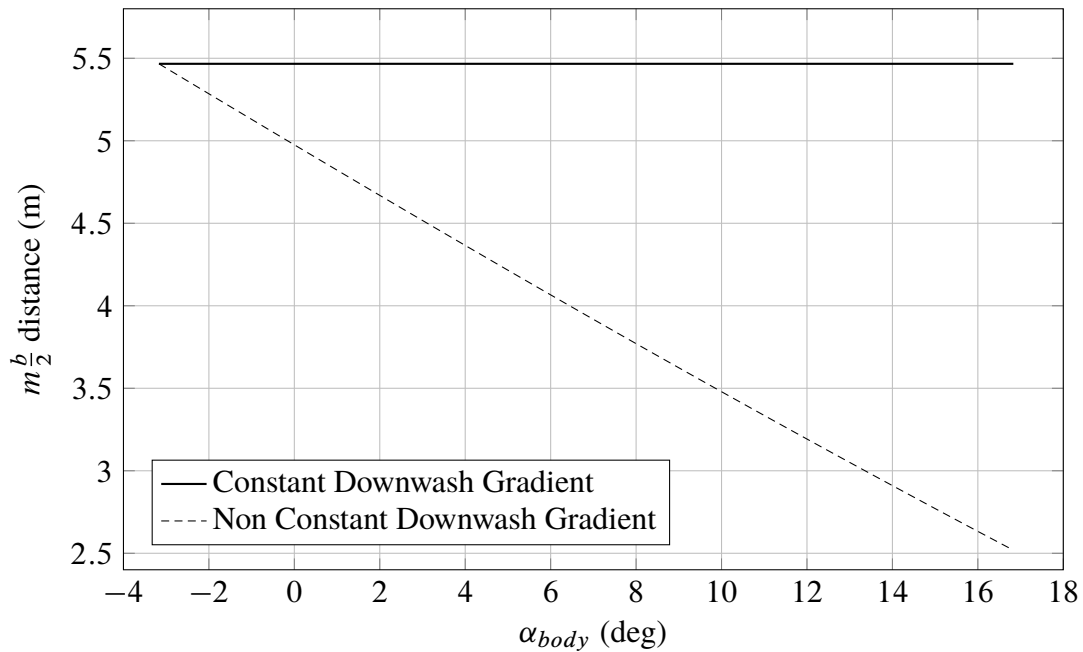


Figure 8.10: ATR 72 Distance between AC horizontal tail and vortex plane vs α_B .

Chapter 9

Aircraft Longitudinal Static Stability

*For every bad thing in life,
there are more good things to tip the balance.*
– Richelle Mead

Static stability is the reaction of a body to a disturbance from equilibrium. To determine the static stability of a body, the body must be initially disturbed from its equilibrium state. If, when disturbed from equilibrium, the initial tendency of the body is to return to its original equilibrium position, the body displays positive static stability or is stable. If the initial tendency of the body is to remain in the disturbed position, the body is said to be neutrally stable. However, should the body, when disturbed, initially tend to continue to displace from equilibrium, the body has negative static stability or is unstable. [21]
In addition to the static stability it's possible to analyze the dynamical stability that is the time history of an aircraft response after it has been disturbed. A statically stable aircraft may not be dynamically stable, as explained in subsequent discussions. However, it is clear that a statically unstable aircraft also is dynamically unstable.

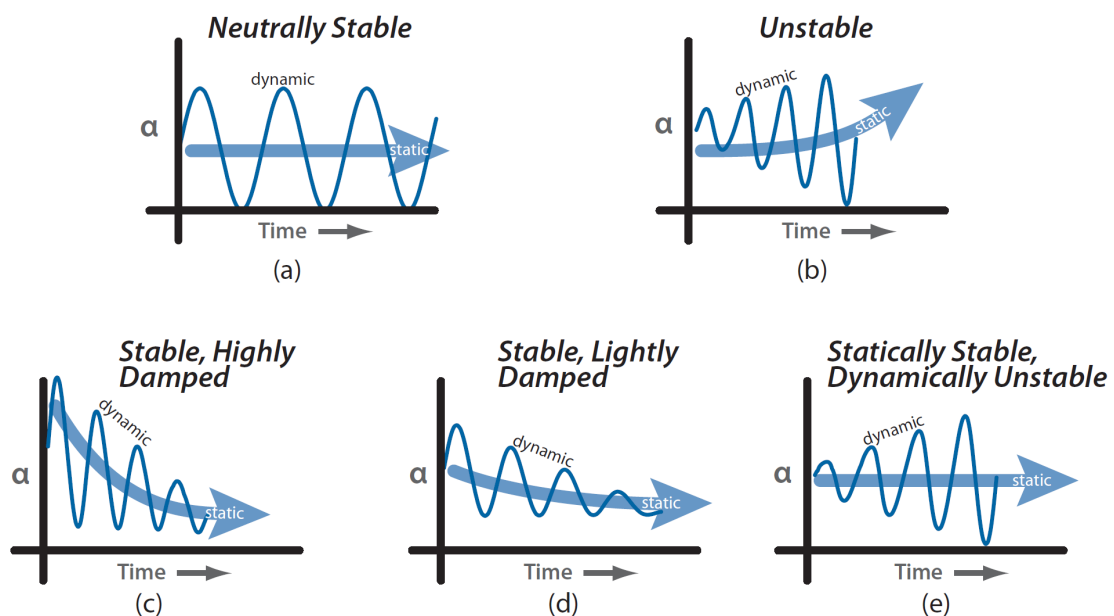


Figure 9.1: Static and dynamic stability about the pitch axis.

It is important to note that there is a substantial difference between the concepts of “Stability” and “Equilibrium”. In fact, stability is a characteristic of an aircraft, while equilibrium is a state in which airplane can be, that means the equilibrium of the forces and the moments acting on it.

“Longitudinal static stability” is the stability of an aircraft in the longitudinal, or pitching, plane under steady-flight conditions. This characteristic is important because an airplane must have the tendency to return to the equilibrium position if perturbed. The pitch plane is the XZ plane of aircraft symmetry. The linear velocities are along the X-axis and w along the Z-axis. Angular velocity is about the Y-axis, known as pitching (positive if nose up). Pilot-induced activation of the elevator changes the aircraft pitch. In the plane of symmetry, the aircraft motion is uncoupled; that is, motion is limited only to the pitch plane.[45]

In order to evaluate the characteristics of longitudinal stability of an aircraft it's necessary to express all the forces and the moments acting on it and evaluate the resultant pitching moment about the center of gravity.

The lift and drag are by definition always perpendicular and parallel to V_∞ , respectively. It is, therefore, inconvenient to use these forces to obtain moments because their moment arms relative to the center of gravity vary with angle-of-attack α . For this reason, all forces are resolved into normal, N, and chordwise, C, forces whose axes remain fixed with the aircraft and whose arms are, therefore, constant. [54]

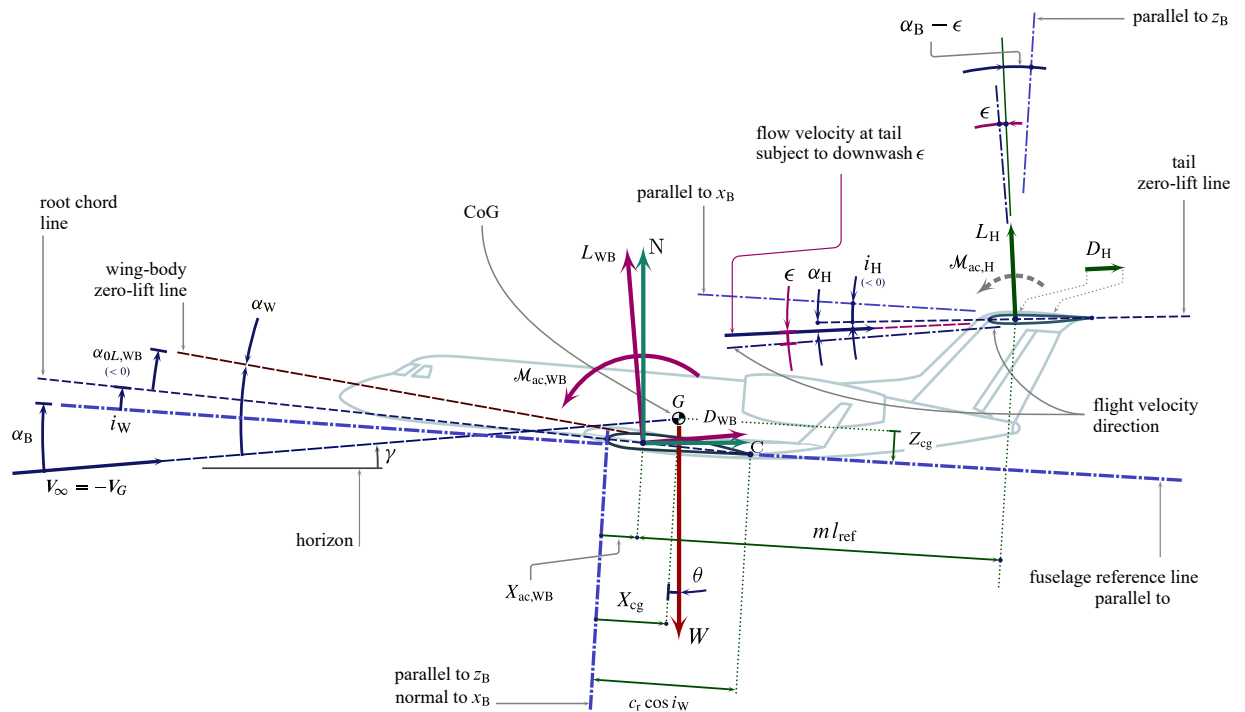


Figure 9.2: Forces and moments acting on an aircraft..

The relation between the lift, the drag and the normal and chordwise forces are the following:

$$N = L \cos(\alpha) + D \sin(\alpha) \quad (9.1)$$

$$C = D \cos(\alpha) - L \sin(\alpha) \quad (9.2)$$

According to what said, the aircraft can, in general, be trimmed, that is, put into an

equilibrium state where the combined lift of the wing and the tail balances the weight while the moment about the center of gravity is zero. It's necessary that this equilibrium point corresponds to positive lift. As regards the stability it is necessary that the response of the aircraft to a disturbance in angle of attack is to tend to return to the original equilibrium position. Thus, if flying in equilibrium at one angle of attack and a disturbance increases the angle of attack, the moment produced at this angle of attack must act to reduce it, that is, tend back toward the original equilibrium state. Conversely, if a disturbance decreases the angle of attack, the moment at the new, lower, angle of attack must serve to increase that angle. This means that the rate of change of the moment about the center of gravity must be negative for static stability: an increase in α should reduce $C_{M_{cg}}$ and a decrease in α should increase $C_{M_{cg}}$. [70] As higher is the slope of the curve, more is greater the the restoring moment. Thus the slope of the curve is called *Static Margin*. Static margin is a concept used to characterize the static longitudinal stability and controllability of aircraft. In aircraft analysis, static margin is defined as the distance between the center of gravity and the neutral point of the aircraft, expressed as a percentage of the mean aerodynamic chord of the wing. In order to have static stability, thus, is necessary that the neutral point is behind the cenetr of gravity.

In conclusion the requirement for static stability are the following:

- The pitching-moment curve exhibit a negative slope
- At a zero angle of attack there is positive nose-up moment

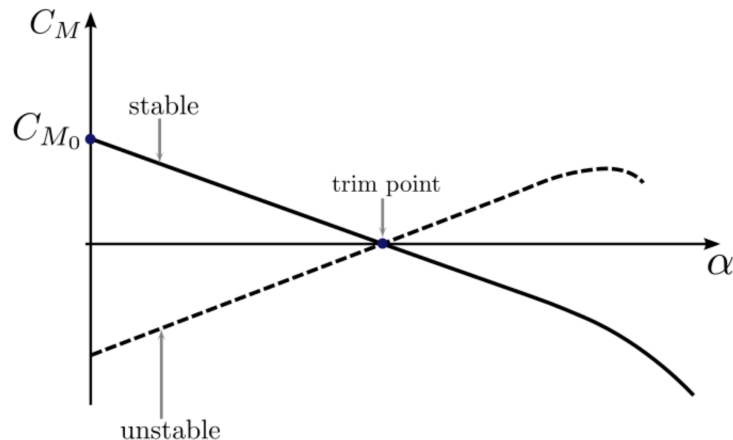


Figure 9.3: Qualitative representation of the moment coefficient vs α .

Below will be calculated all the contributions in order to evaluate the pitching moment coefficient about the center of gravity.

9.1 Aerodynamic Lift

Considering a reference angle of attack α_B , the aircraft components generates lift. So it is necessary to evaluate these contributes. In particular, first of all, is wanted to evaluate the C_L of isolated wing. This value will be correct with fuselage influence. Afterwards it is necessary to evaluate the contribute of horizontal tail. It is important to note that each component works at a different angle of attack in dependence of angles of incidence and downwash , meanwhile for longitudinal stability the reference angle of attack is α_B .

9.1.1 Wing

The wing may be considered as the most important component of an aircraft. Its main purpose is to generate sufficient lift force. However, the wing has two other productions, namely drag force or drag and pitching moment. While a wing designer is looking to maximize the lift, the other two (drag and pitching moment) must be minimized. The theoretical background and the followed process are shown in the CHAPT 6.

9.1.2 Fuselage

The fuselage is that portion of the aircraft wherein the payload is carried. In jet transports the payload consists of the passengers and their baggage and/or cargo. It is important that the fuselage has some features as a low aerodynamic drag; a minimum aerodynamic instability; comfort and attractiveness in terms of seat design, placement, and storage space; safety during emergencies; minimization of noise and ease of cargo handling in loading and unloading.[70]

The lift distribution on a wing is affected by the presence of the fuselage as a result of the following effects:

- The presence of the fuselage disturbs the longitudinal velocity field near the wing.
- At an angle of attack relative to the free stream, the fuselage also perturbs the flow about the wing in planes normal to the free stream.
- The fuselage has a blocking effect on the flow.

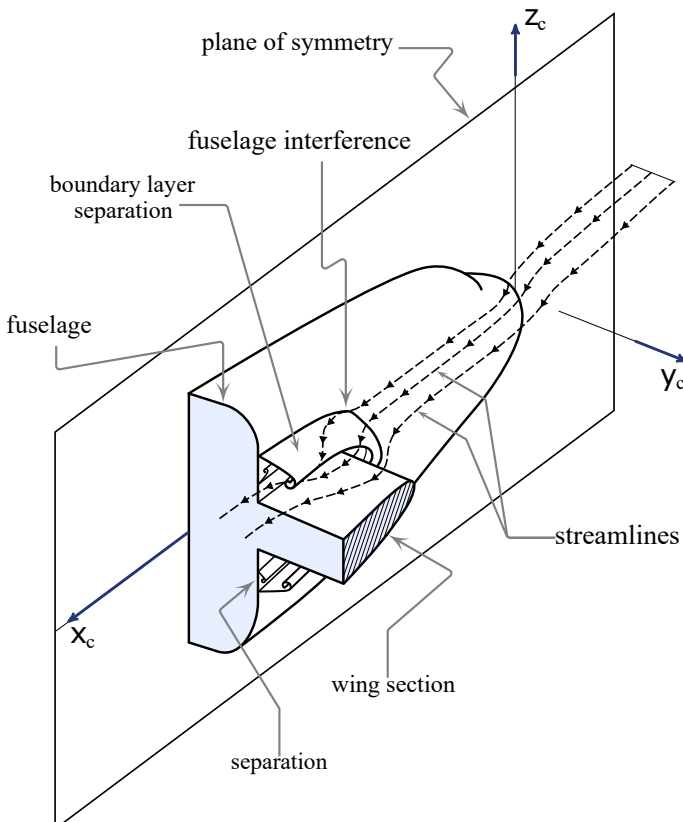


Figure 9.4: Wing fuselage junction flow.

These effects are not large for a slender fuselage but may be important when the fuselage is relatively bulky, so that a substantial alteration to the local longitudinal velocity may result. The cross-flow caused by the fuselage at angle of attack changes the component of free stream velocity normal to the fuselage axis and affects the downwash flow produced by the wing. The blocking effect of the fuselage is always present even if the fuselage is an infinite cylinder aligned with the free stream, in which case the other two effects are not present. [70]

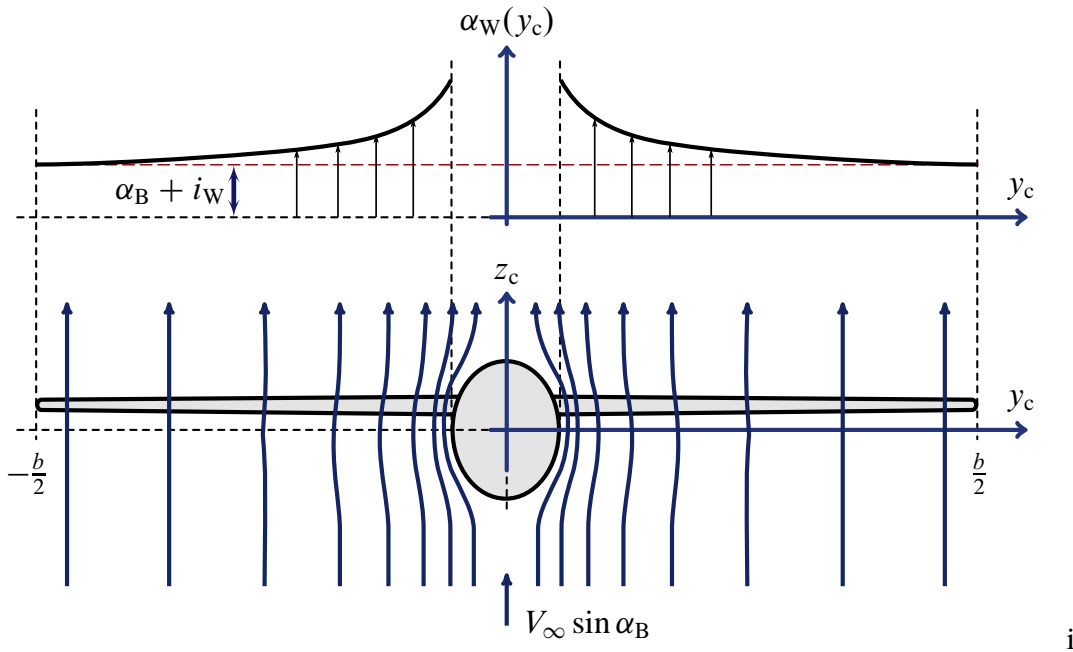


Figure 9.5: Wing fuselage front view interference.

However, theoretical analysis showed that the presence of a slender fuselage does not have an important effect on the lift distribution on an unswept wing of moderate aspect ratio, but a larger change in the lift distribution on a wing in the presence of a fuselage may be anticipated if the wing is swept.[72] For greater accuracy of the calculation, the value of lift linear slope has been corrected using the following equation from [66]:

$$\left(\frac{dC_L}{d\alpha} \right)_{wb} = \left[1 + \frac{1}{4} \left(\frac{d}{b} \right) - \frac{1}{40} \left(\frac{d}{b} \right)^2 \right] \left(\frac{dC_L}{d\alpha} \right)_w \quad (9.3)$$

Note that for typical airliners $\frac{d}{b} \approx 0.1$ and therefore the lift curve slope of the wing-body is approximately equal to that of the wing alone.

In addition to the calculation of the linear slope of the wing body group, it is necessary to calculate the intersection point between the lift curve of wing and the lift curve of wing-body. This point is the α_{0L} of the exposed wing. The exposed wing is the part of wing outside of the fuselage that generates lift in a complete aircraft. This value has been calculated with the following integral formula.

$$\alpha_{0L}|_{EW} = \frac{2}{S_E} \int_{y_{0E}}^{\frac{b}{2}} c(y)[\alpha_0(y_E) - \epsilon_T(y_E)] dy \quad (9.4)$$

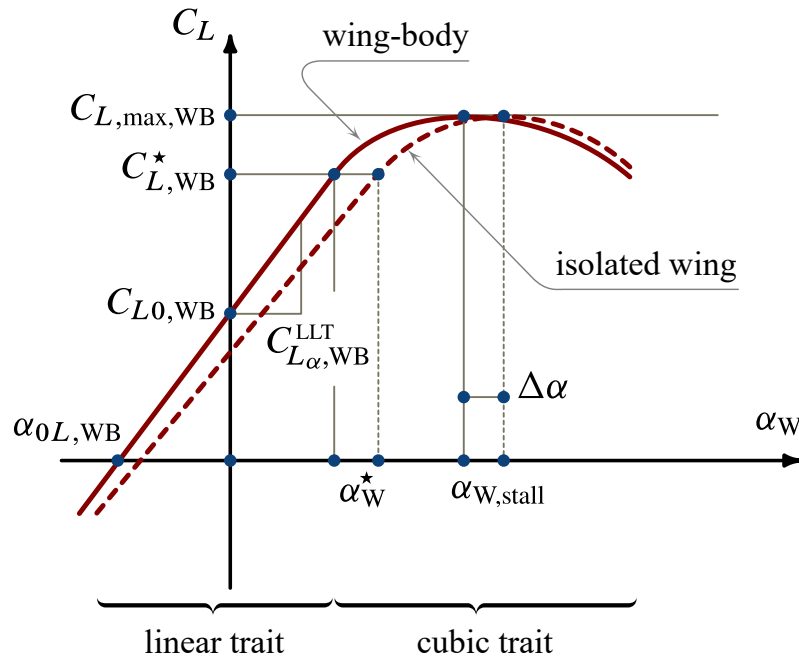


Figure 9.6: Lift curve of isolated wing and of wing-body group.

9.1.3 Horizontal Tail

The horizontal tail is an aerodynamic surface, typically including one or more movable control surfaces, that provides longitudinal stability and control. A stabilizer can feature a fixed or adjustable structure on which any movable control surfaces are hinged, or it can itself be a fully movable surface. In the first case the horizontal tail consists of the *stabilizer* and the *elevator* (moving) for handling the pitch degree of freedom. In case of a fully movable surface it is called *stabilator*.

The H-tail can be positioned low through the fuselage, in the middle cutting through the V-tail, or at the top of the V-tail to form a T-tail. [45] The horizontal tail provides longitudinal stability and control. It may be sized by one or more of the following conditions[56]:

- Provide static and dynamic stability. Provide a state of equilibrium in each flight condition.
- Enable aircraft control.
- Provide a state of equilibrium in each flight condition.

The stabilizer is a fixed wing section whose job is to provide stability for the aircraft, to keep it flying straight. The horizontal stabilizer prevents up-and-down, or pitching, motion of the aircraft nose. The elevator is the small moving section at the rear of the stabilizer that is attached to the fixed sections by hinges. Because the elevator moves, it varies the amount of force generated by the tail surface and is used to generate and control the pitching motion of the aircraft. There is an elevator attached to each side of the fuselage. The elevators work in pairs; when the right elevator goes up, the left elevator also goes up.

Considering an horizontal tail formed by stabilizer and elevator, in order to evaluate the lift coefficient of this lifting surface it's necessary to consider the deflection of control surface. The elevator, in fact, can be considered as a *plain flap*.

Elevator index of effectiveness

In order to evaluate the contribution to the longitudinal stability of horizontal tail it's necessary to consider the deflection of the elevator.

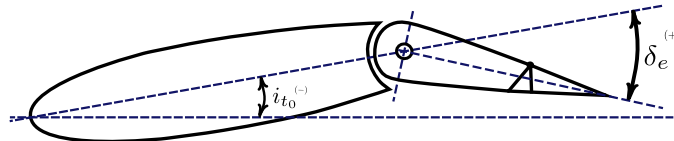


Figure 9.7: Characteristic angles of the horizontal tail.

The variation of zero lift angle is not constant with the angle of deflection. So it's necessary to evaluate the tau factor which is defined as follows:

$$\tau_e = \frac{d\alpha_{0l}}{d\delta_e} \quad (9.5)$$

Introducing this parameter the lift coefficient of the horizontal tail can be rated as follows:

$$C_{L_H} = C_{L_0} + C_{L_{\alpha_H}} \alpha_H + C_{L_{\alpha_H}} \tau_e \delta_e \quad (9.6)$$

Considering a symmetrical horizontal tail, the term C_{L_0} is zero, so it's possible to express the lift coefficient in the following form:

$$C_{L_H} = C_{L_{\alpha_H}} (\alpha_H + \tau_e \delta_e) \quad (9.7)$$

In general the value of τ is constant until about 15 deg; after this value, due to the flow separation, the effectiveness of elevator decrease and consequently the product $\tau_e \delta_e$ that appears in the equation of lift coefficient.

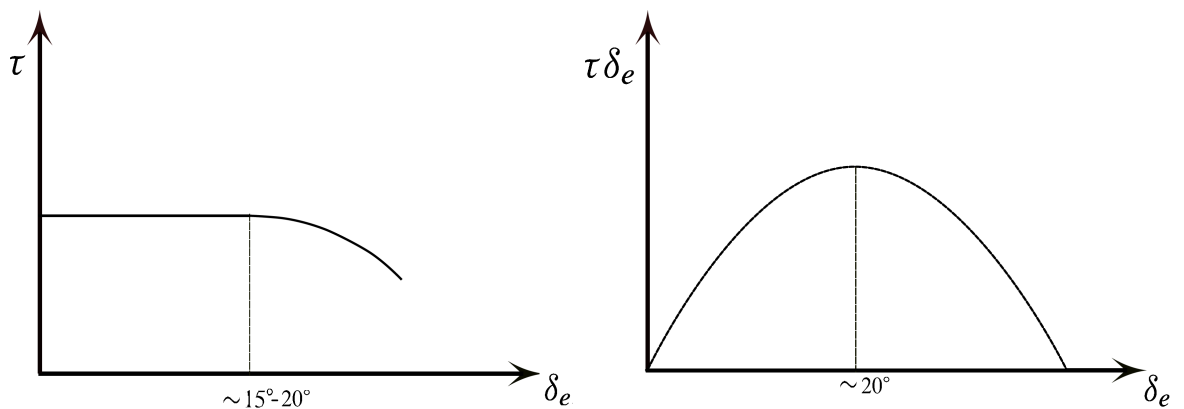


Figure 9.8: Qualitative trend of τ with the deflection of elevator.

Figure 9.9: Qualitative trend of the term $\tau \cdot \delta_e$ with the deflection of elevator.

The evaluation of tau is made by reading of external database, considering the following graphs.

$$\tau = \alpha_\delta \eta_\delta = \frac{\alpha_{\delta_{cL}}}{\alpha_{\delta_{cL}}} \alpha_{\delta_{cL}} \eta_\delta \quad (9.8)$$

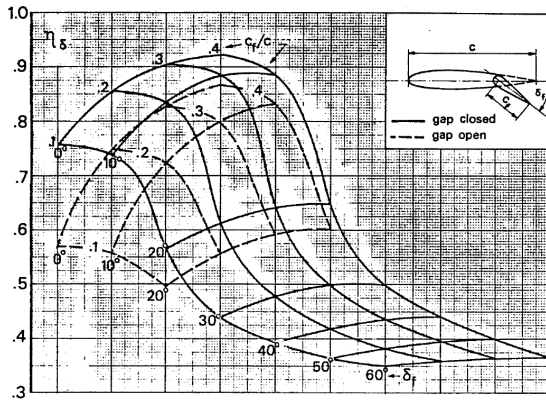


Figure 9.10: 2D efficiency correction for elevator.

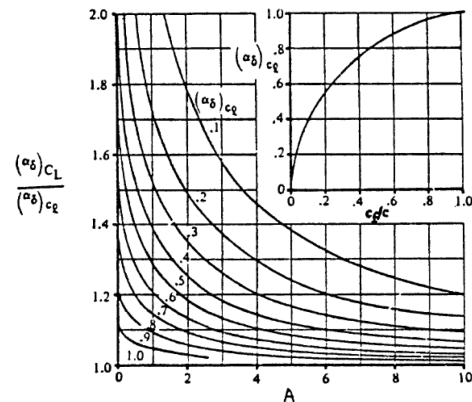


Figure 9.11: $\frac{d\alpha_{0L}}{d\delta_e}$ 2D and 3D correction.

9.1.4 Complete Aircraft

In order to evaluate the lift coefficient of the entire airplane it's possible to consider it as consisting of the following parts[63]:

- Wing and Fuselage
- Horizontal Tail
- Canard

It's important to consider the effectiveness angles of attack in which the surfaces work. This is made considering the angles of incidence of the lifting surfaces and the downwash angle aft of the wing. An horizontal tail and a canard may be equipped with a trailing edge control surface. So in order to evaluate these contributes it's important to know the angle of deflection δ of these control surfaces.

The calculation of the individual contributions it's reported in the relevant sections. In this section will be shown the method to evaluate the aircraft lift coefficient, known the single contributes.

For an aircraft with no canard, the formula is the following:

$$C_L = C_{L_{wb}} + \frac{S_t}{S_w} \eta_t C_{L_t} \quad (9.9)$$

Where η_t is the ratio of dynamic pressure, called *tail efficiency factor*. In fact the dynamic pressure seen by horizontal tail differ from the free stream dynamic pressure due to two main reasons: the combination wing-fuselage and the presence of the propeller. The dynamic pressure of the tail depends on the location of the tail. If the tail is in the wake of the wing-body, the local dynamic pressure will be less than the freestream because the flow gradually loses its kinetic energy. While if the tail is in the slipstream of propeller, the local dynamic pressure may increase due to the power absorbed by the propeller.

9.2 Aerodynamic Drag

The drag of an aircraft depends on its shape and speed, which are design-dependent, as well as on the properties of air, which are nature-dependent. Drag is a complex phenomenon arising from several sources, such as the viscous effects that result in skin friction and pressure

differences as well as the induced flow field of the lifting surfaces and compressibility effects. The aircraft drag estimate starts with the isolated aircraft components. Each component of the aircraft generates drag largely dictated by its shape. Total aircraft drag is obtained by summing the drag of all components plus their interference effects when the components are combined. It is important to note that the drag of two isolated bodies increases when they are brought together due to the interference of their flow fields.[45]

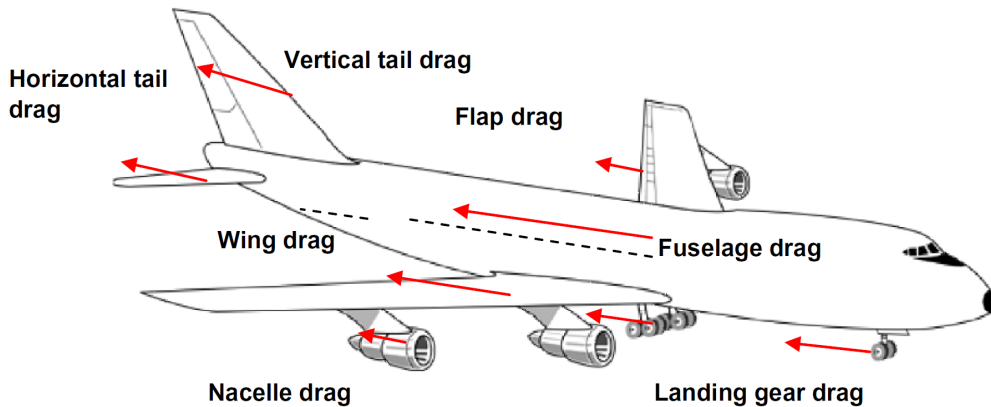


Figure 9.12: Drag components making up the total commercial airplane drag.[70]

In this thesis work, in order to evaluate the pitching moment coefficient of an aircraft has been considered the drag forces due to wing and horizontal tail.

9.2.1 Drag of a lifting surface

As widely expressed in the CHAPT 7, the drag coefficient of a lifting surface is calculated starting from the drag coefficient of the airfoils, expressed by the following equation:

$$CD = CD_{min} + (CL - CL_{CD_{min}})^2 + k \quad (9.10)$$

For each station, known the semi-spanwise lift distribution, it's possible to calculate the local lift coefficient of the intermediate airfoil and, consequently, the drag coefficient. After the drag coefficient of the entire lifting surface is calculated with an integral.

9.2.2 Additional drag due to elevator

For the horizontal tail it's necessary to consider the additional drag due to the elevator deflection. It's possible to consider the elevator as a *plain flap* and use the concerning methods.

A plain flap is an high lift devices where a portion of the rear of a wing is simply hinged. The effectiveness of the flap derives from the fact that on rotation it changes the camber of the section and so permits of a change of circulation and therefore, of lift at a given incidence. The increment in profile drag coefficient due to a flap at a given incidence is rather more influenced by test conditions than is the lift coefficient increment. Nevertheless, the influence of test conditions and wing incidence is still sufficiently small over a wide range of incidence for us to accept the increment at a standard incidence as a reliable measure of the profile drag characteristics of a flap. [78] The increment of drag is a ΔCD_0 Young and Hufton assumed that ΔCD_0 can be calculated as follow for a full-span flap:

$$\Delta CD_0 = \delta_1 (c_f/c) \cdot \delta_2 (\delta_f) \quad (9.11)$$

where δ_1 and δ_2 are functions that were determined from experimental data. Their related curves are shown in figure 9.13 and 9.14 for plain flap.

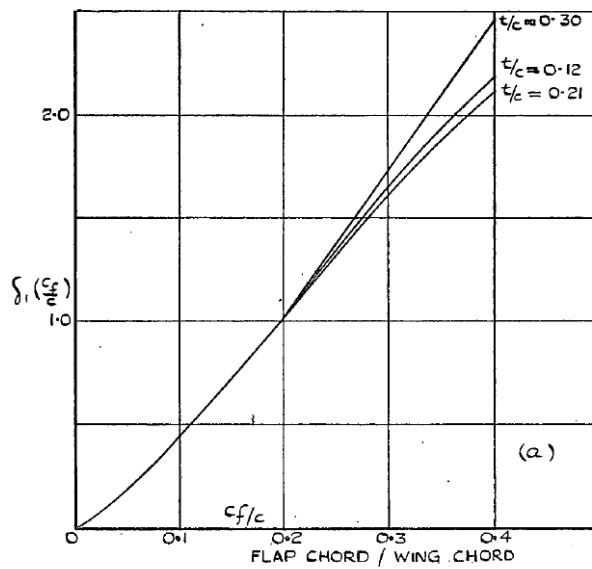


Figure 9.13: The functions $\delta_1 (c_f/c)$ for split and plain flaps

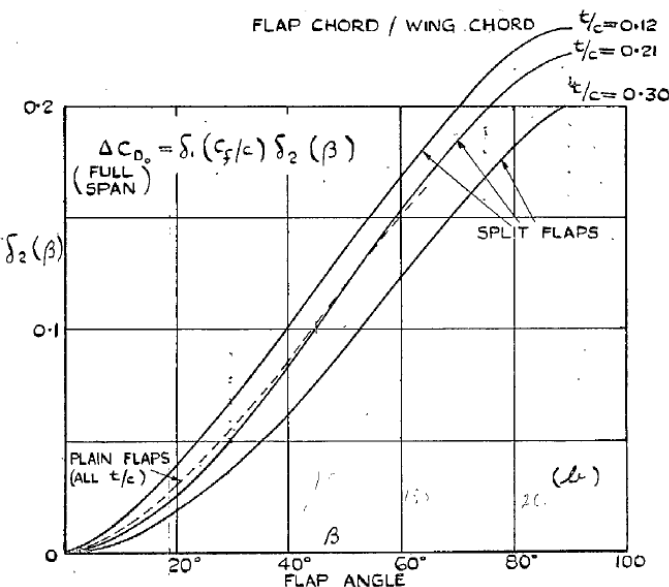


Figure 9.14: The functions $\delta_2 (\delta_f)$ for plain flaps

9.3 Pitching Moments

The purpose of this section is to explain the followed procedure used to evaluate the pitching coefficient moments of the aircraft components.

Due to the interaction between the body and the flow a pressure distribution is generated whose result is the aerodynamic force acting at the center of pressure. In consequence of what there is a pitching moment that is a moment acting on the pitch axis of a moving body. As angle of attack changes on a cambered airfoil, there is movement of the center of pressure forward and aft. One of the remarkable properties of a cambered airfoil is that, even though

the center of pressure moves forward and aft, there is a point, called Aerodynamic Center, with respect to which the moment coefficient is constant. The aerodynamic center is the most convenient place to locate the lift, drag, and moment of an aircraft wing or airfoil section. So, for each component of the aircraft, it will be calculated the pitching moment coefficient respect to its aerodynamic center.

9.3.1 Lifting surface

In order to evaluate the pitching moment coefficient of a lifting surface, at a given angle of attack, the implemented process is the following.

First it's calculated the pitching moment coefficient respect to the point at a quarter of the mean aerodynamic chord. Starting from these values, to vary the angle of attack, it's possible to evaluate the position of aerodynamic center.

1. Fifty points along the semispan are defined
2. For each point, an intermediate airfoil is calculated
3. For each airfoil, at given station, the lift coefficient is calculated with the local CL vs α curve. In this way it's possible to consider both the linear trait and non linear
4. For each airfoil the center of pressure is calculated using the following equation:

$$\frac{x_{CP}}{c} = \frac{x_{AC}}{c} - \frac{C_{Mac}}{C_l} \quad (9.12)$$

5. For each airfoil the arm between the local center of pressure and the point at a quarter of lifting surface's MAC is calculated. The equations that define the MAC are the following:

$$MAC = \frac{2}{S} \int_0^{\frac{b}{2}} c^2 dy \quad (9.13)$$

$$x_{MAC} = \frac{2}{S} \int_0^{\frac{b}{2}} x_{le}(y)c(y) dy \quad (9.14)$$

$$y_{MAC} = \frac{2}{S} \int_0^{\frac{b}{2}} y_{le}(y)c(y) dy \quad (9.15)$$

6. Finally it's possible to evaluate the pitching moment respect to the point at a quarter of MAC with the product between the lift force and the arm

Repeating the process to vary the angle of attack it's possible to estimate the slope of the pitching moment curve. In fact, the aerodynamic center, is that point on an aircraft, wing, or airfoil section about which the pitching moment is independent of angle of attack. If the slope is positive, the aerodynamic center is behind the quarter of the MAC, conversely if the slope is negative, the aerodynamic center is the quarter of the MAC is behind the aerodynamic center.

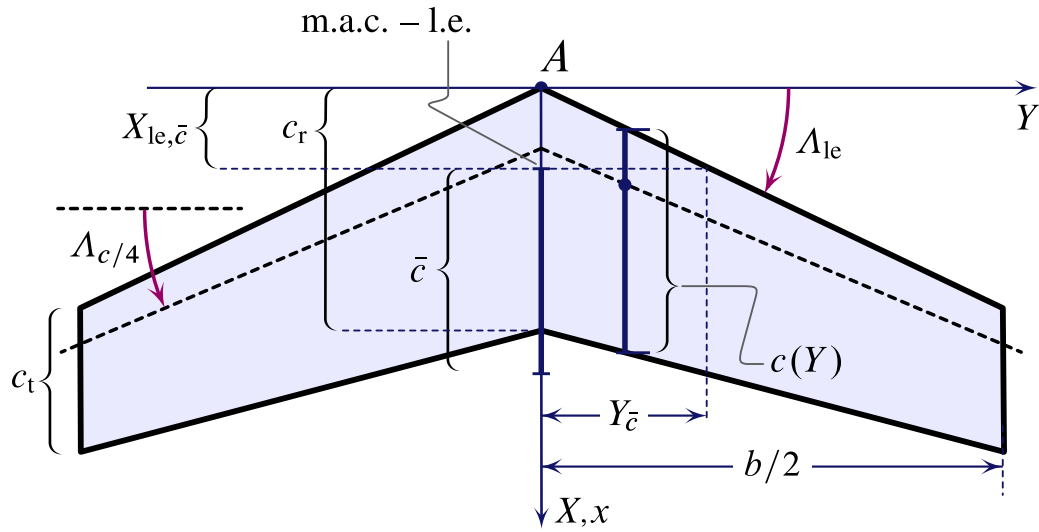


Figure 9.15: Wing topview definitions.

9.3.2 Fuselage

The moment coefficient of the fuselage is a pure couple, so is not necessary specify the pole.

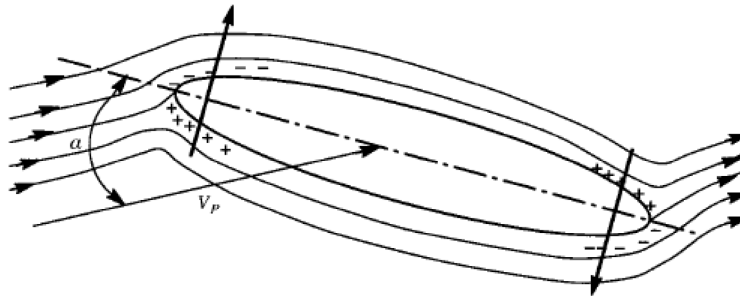


Figure 9.16: Fuselage in potential flow at angle of attack.

Assuming the linearity, is possible to represent the pitching moment coefficient by the following equation in function of the angle of attack.

$$C_{M_f} = C_{M_{0f}} + C_{M\alpha_f} \alpha_{body} \quad (9.16)$$

In JPAD it's possible to evaluate these two contributes using different methods.

Multhopp method

Each term in the equation 9.16 can be calculated by the Multhopp method. The fuselage is divided into strips, each of which gives a contribution to the pitching moment according to its distance from the wing.

The two coefficients $C_{M_{0f}}$ and $C_{M\alpha_f}$ in eq. 9.16 can be obtained from the following equations.

$$C_{M_{0f}} = \frac{K_2 - K_1}{36.5 \cdot S \cdot MAC} \cdot \int_0^{l_f} W_f^2 \cdot (\alpha_{0Lw} + i_w + i_{cl_f}) \, dx \quad (9.17)$$

$$C_{M\alpha_f} = \frac{1}{36.5 \cdot S \cdot MAC} \cdot \left\{ \int_0^{l_f 1} W_f^2 \cdot \left[\left(\frac{\partial \epsilon_u}{\partial \alpha} \right)_1 + 1 \right] dx_1 + \int_0^{l_f 2} W_f^2 \cdot \left[\left(\frac{\partial \epsilon_d}{\partial \alpha} \right)_2 + 1 \right] dx_2 \right\} \quad (9.18)$$

Instead of the integrals it's possible to substitute them with summations.

$$C_{M0f} = \frac{K_2 - K_1}{36.5 \cdot S \cdot MAC} \cdot \sum_{j=1}^n W_{f_j}^2 \cdot (\alpha_{0Lw} + i_w + i_{cl_f}) \cdot \Delta x; \quad (9.19)$$

$$C_{M\alpha_f} = \frac{1}{36.5 \cdot S \cdot MAC} \cdot \left\{ \sum_{j=1}^{n_1} W_{f_j}^2 \cdot \left[\left(\frac{\partial \epsilon_u}{\partial \alpha} \right)_1 + 1 \right] \cdot \Delta x_1 + \sum_{j=1}^{n_2} W_{f_j}^2 \cdot \left[\left(\frac{\partial \epsilon_d}{\partial \alpha} \right)_2 + 1 \right] \cdot \Delta x_2 \right\} \quad (9.20)$$

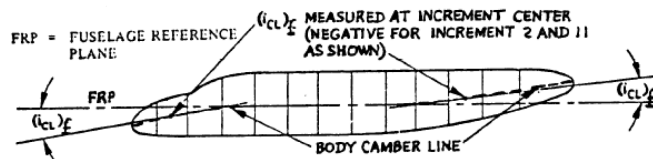


Figure 9.17: Strips definition for the determination of C_{M0f} .

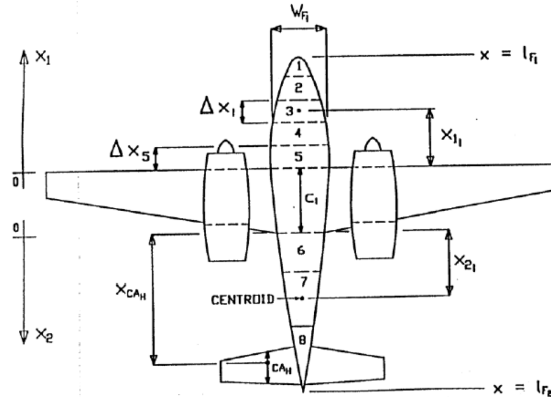


Figure 9.18: Strips definition for the determination of $C_{M\alpha_f}$.

The parameter $K_2 - K_1$ is a correction factor that is dependent on the value of the fineness ratio and is evaluated by the following figure.[25]

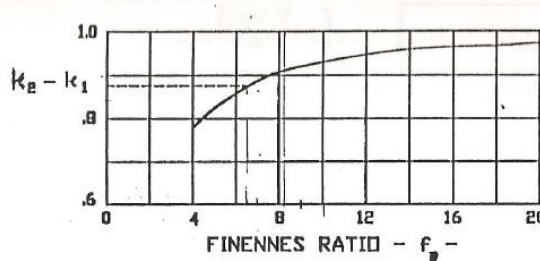


Figure 9.19: $K_2 - K_1$ correction factor in function of fineness ratio.

For stability it's necessary to evaluate the new aerodynamic center (wing-body) and the pitching moment coefficient respect to this point. In fact the fuselage introduces a shift of the aerodynamic center to the leading edge. It's possible to obtain the new aerodynamic center using the Eq. 9.21

$$\Delta X_{ac} = x_{ac_{wb}} - x_{ac_w} = -\frac{C_{M_{\alpha_f}}}{C_{L_{\alpha_f}}} \quad (9.21)$$

The wing-body pitching moment respect to the new aerodynamic center is :

$$C_{M_{ac_{wb}}} = C_{M_{ac_w}} + C_{M_{0f}} \quad (9.22)$$

Fuselage Pitching moment prediction method

This method has been developed in the Dept. of Industrial Engineering, University of Study of Naples Federico II, by numerical aerodynamic analyses performed with STAR-CCM+. From a reference fuselage layout the nose, cabin (constant fuselage diameter), and tailcone geometry have been parametrically changed. Then, the aerodynamic drag, the pitching moment at zero incidence, the longitudinal static stability derivative, and the yawing moment coefficients C_D , C_{M_0} , C_{M_α} , and C_{N_β} respectively, have been evaluated by numerical analysis. Aerodynamic effects of each component (nose, cabin, tailcone) have been directly obtained from the CFD aerodynamic solver, separating the forces and moments contributions of each fuselage part. [4]

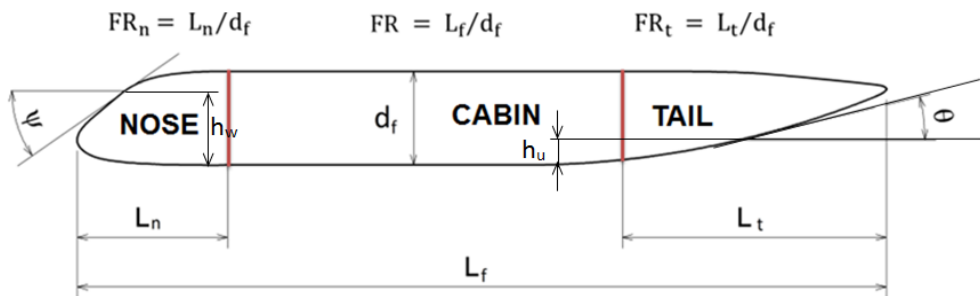


Figure 9.20: Main fuselage geometrical parameters.

The fuselage pitching moment coefficient can be estimated according to the equation 9.16 where :

$$C_{M_{0f}} = C_{M_{0FR}} + \Delta C_{M_{0NOSE}} + \Delta C_{M_{0TAIL}} \quad (9.23)$$

$$C_{M_{\alpha_f}} = C_{M_{\alpha FR}} + \Delta C_{M_{\alpha NOSE}} + \Delta C_{M_{\alpha TAIL}} \quad (9.24)$$

where the subscript *FR* refers to the pitching moment coefficient as function of fuselage fineness ratio. The subscript *NOSE* the pitching moment nose correction factor. It depends on windshield angle Φ and on the nose fineness ratio FR_n . Finally the subscript *TAIL* refers to the pitching moment tail correction factor. It depends on upsweep angle θ and on the tail fineness ratio FR_t .

The following figures show the variability of introduced parameters.

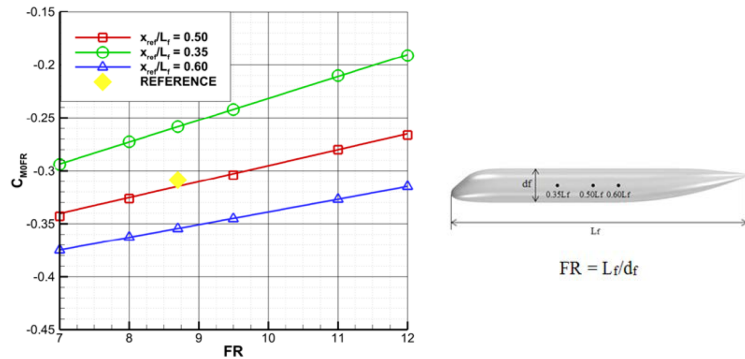


Figure 9.21: Zero angle of attack pitching moment coefficient $C_{M0,FR}$.

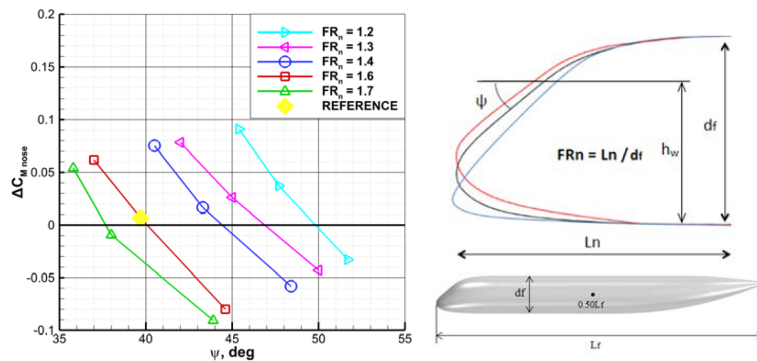


Figure 9.22: Zero angle of attack pitching moment coefficient nose correction factor.

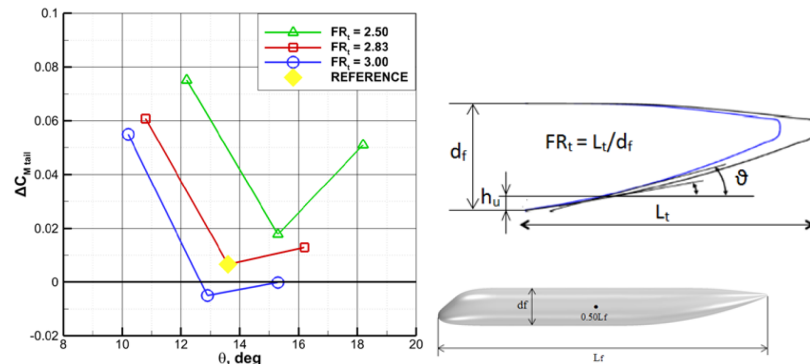


Figure 9.23: Zero angle of attack pitching moment coefficient tail correction factor.

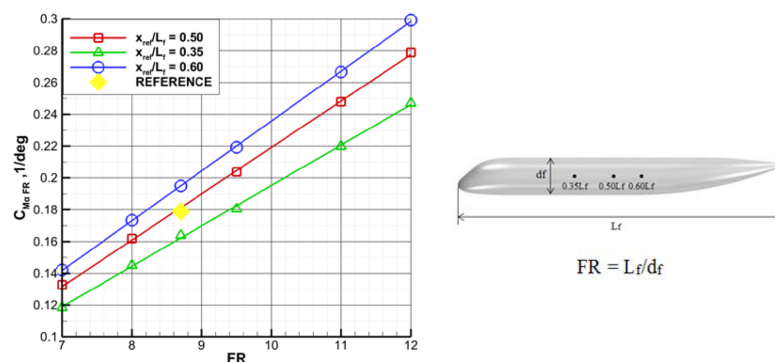


Figure 9.24: Pitching moment derivative with respect to FR.

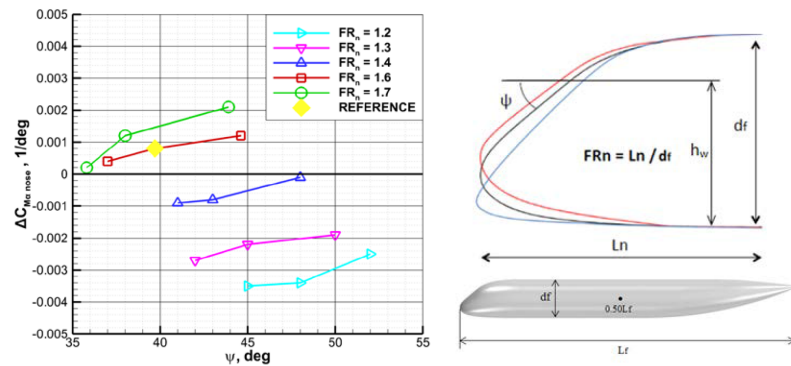


Figure 9.25: Pitching moment derivative nose correction factor.

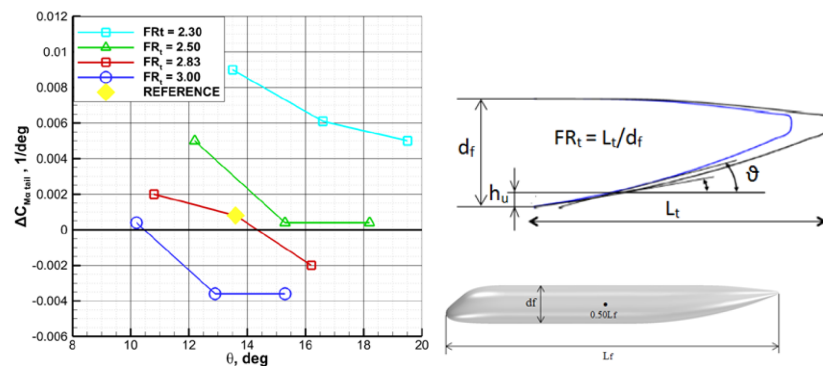


Figure 9.26: Pitching moment derivative tail correction factor.

9.4 Propulsors

9.4.1 Stability Calculation

9.4.2 Neutral Point and Static Margin

9.5 Java Class Architecture

9.6 Case Study

Chapter 10

Minor Works

Appendices

Appendix A

HDF dataset and database reader creation

In a tool for preliminary design phase of an aircraft, it's very important to have available database. It's possible to create database starting from graphics using external software. In this appendix will be explained the step required in order to digitalize the graphics, create an HDF dataset and set up the database-reader class in Jpad.

A.1 Chart Digitization

The first step required for create a dataset is to digitalize a chart. Often data is found presented in reports and references as functional X-Y type scatter or line plots. In order to use this data, it must somehow be digitized. This is made with an external software, such as *Plot Digitizer*. Plot Digitizer is a Java program used to digitize scanned plots of functional data. This program will allow you to take a scanned image of a plot (in GIF, JPEG, or PNG format) and quickly digitize values off the plot just by clicking the mouse on each data point.[14]

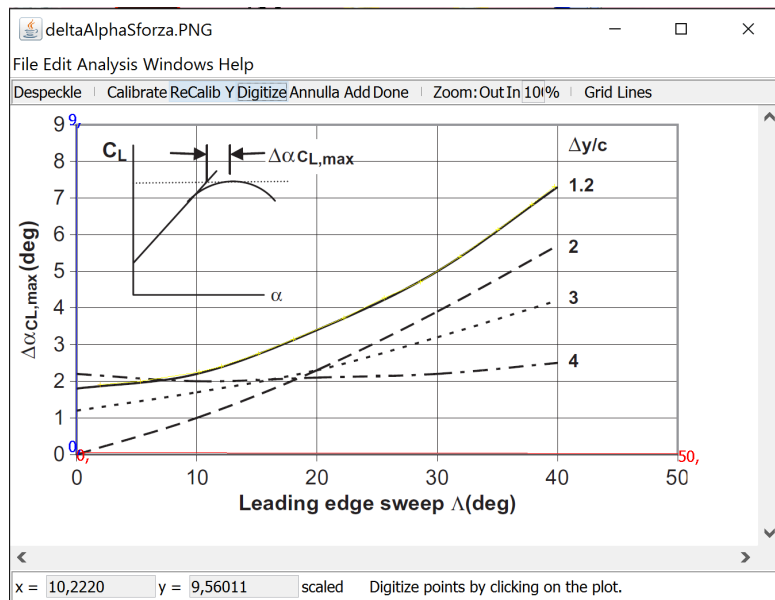


Figure A.1: Chart digitization using Plot Digitizer.

In order to digitize a chart, first of all it's necessary to calibrate the axis. Plot Digitizer works with both linear and logarithmic axis scales. After it's possible to digitize a curve

simply click on it. The values obtained can then be saved to a tex file or .csv file.

A.2 Creation of an HDF file with Matlab

Obtained the .csv file from digitization is necessary to create the HDF file. First of all it's necessary to import the file with couple of coordinates as matrix. After saving the imported files as .mat file, Matlab code comes in play to manage these data and to generate the digitalized curves and the HDF dataset. The code interpolates curves points with cubic splines in order to have more points to plot for each curve.

Listing A.1 MATLAB script for creating the HDF Database

```

clc; close all; clear all;

%% Import data
DeltaAlphaCLmax_vs_LambdaLE_dy1p2 = importdata('DeltaAlphaCLmax_vs_LambdaLE_dy1p2.mat');
DeltaAlphaCLmax_vs_LambdaLE_dy2p0 = importdata('DeltaAlphaCLmax_vs_LambdaLE_dy2p0.mat');
DeltaAlphaCLmax_vs_LambdaLE_dy3p0 = importdata('DeltaAlphaCLmax_vs_LambdaLE_dy3p0.mat');
DeltaAlphaCLmax_vs_LambdaLE_dy4p0 = importdata('DeltaAlphaCLmax_vs_LambdaLE_dy4p0.mat');

nPoints = 30;
lambdaLEVector_deg = transpose(linspace(0, 40, nPoints));

%% dy/c = 1.2
smoothingParameter = 0.999999;
DAlphaVsLambdaLESplineStatic_Dy1p2 = csaps( ...
    DeltaAlphaCLmax_vs_LambdaLE_dy1p2(:,1), ...
    DeltaAlphaCLmax_vs_LambdaLE_dy1p2(:,2), ...
    smoothingParameter ...
);

DAlphaVsLambdaLESplineStatic_Dy1p2 = ppval( ...
    DAlphaVsLambdaLESplineStatic_Dy1p2, ...
    lambdaLEVector_deg ...
);

%% dy/c = 2.0
smoothingParameter = 0.999999;
DAlphaVsLambdaLESplineStatic_Dy2p0 = csaps( ...
    DeltaAlphaCLmax_vs_LambdaLE_dy2p0(:,1), ...
    DeltaAlphaCLmax_vs_LambdaLE_dy2p0(:,2), ...
    smoothingParameter ...
);

DAlphaVsLambdaLESplineStatic_Dy2p0 = ppval( ...
    DAlphaVsLambdaLESplineStatic_Dy2p0, ...
    lambdaLEVector_deg ...
);

%% dy/c = 3.0
smoothingParameter = 0.999999;
DAlphaVsLambdaLESplineStatic_Dy3p0 = csaps( ...
    DeltaAlphaCLmax_vs_LambdaLE_dy3p0(:,1), ...
    DeltaAlphaCLmax_vs_LambdaLE_dy3p0(:,2), ...
    smoothingParameter ...
);

DAlphaVsLambdaLESplineStatic_Dy3p0 = ppval( ...
    DAlphaVsLambdaLESplineStatic_Dy3p0, ...
    lambdaLEVector_deg ...
);

%% dy/c = 4.0
smoothingParameter = 0.999999;
DAlphaVsLambdaLESplineStatic_Dy4p0 = csaps( ...
    DeltaAlphaCLmax_vs_LambdaLE_dy4p0(:,1), ...
    DeltaAlphaCLmax_vs_LambdaLE_dy4p0(:,2), ...
);

```

```

smoothingParameter ...  

);  
  

DAlphaVsLambdaLEStatic_Dy4p0 = ppval( ...  

    DAlphaVsLambdaLESplineStatic_Dy4p0, ...  

    lambdaLEVector_deg ...  

);  
  

%% Plots  

figure(1)  

plot ( ...  

    lambdaLEVector_deg, DAlphaVsLambdaLEStatic_Dy1p2, '-*b' ... , ...  

);  

hold on  
  

plot ( ...  

    lambdaLEVector_deg, DAlphaVsLambdaLEStatic_Dy2p0, '-b' ... , ...  

);  

hold on  
  

plot ( ...  

    lambdaLEVector_deg, DAlphaVsLambdaLEStatic_Dy3p0, '*b' ... , ...  

);  

hold on  
  

plot ( ...  

    lambdaLEVector_deg, DAlphaVsLambdaLEStatic_Dy4p0, 'b' ... , ...  

);  
  

xlabel('\Lambda_{le}_{(deg)}'); ylabel('Delta\alpha_{C_{L,max}}');  

title('Angle_of_attack_increment_for_wing_maximum_lift_in_subsonic_flight');  

legend('\Delta_y/c=1.2', '\Delta_y/c=2.0', '\Delta_y/c=3.0', '\Delta_y/c=4.0');  

axis([0 50 0 9]);  

grid on;  
  

%% preparing output to HDF  
  

% dy/c  

dyVector = [ ...  

    1.2; 2.0; 3.0; 4.0 ...  

];  
  

%columns --> curves  

myData = [ ...  

    DAlphaVsLambdaLEStatic_Dy1p2, ...  

    DAlphaVsLambdaLEStatic_Dy2p0, ... % -> 2  

    DAlphaVsLambdaLEStatic_Dy3p0, ... % -> 3  

    DAlphaVsLambdaLEStatic_Dy4p0]; % -> 4  
  

hdfFileName = 'DAlphaVsLambdaLEVsDy.h5';  
  

if ( exist(hdfFileName, 'file') )  

    fprintf('file %s exists, deleting and creating a new one\n', hdfFileName);  

    delete(hdfFileName)  

else  

    fprintf('Creating new file %s\n', hdfFileName);  

end  
  

% Dataset: data  

h5create(hdfFileName, '/DAlphaVsLambdaLEVsDy/data', size(myData));  

h5write(hdfFileName, '/DAlphaVsLambdaLEVsDy/data', myData);  
  

% Dataset: var_0  

h5create(hdfFileName, '/DAlphaVsLambdaLEVsDy/var_0', size(dyVector));  

h5write(hdfFileName, '/DAlphaVsLambdaLEVsDy/var_0', dyVector);  
  

% Dataset: var_1  

h5create(hdfFileName, '/DAlphaVsLambdaLEVsDy/var_1', size(lambdaLEVector_deg));  

h5write(hdfFileName, '/DAlphaVsLambdaLEVsDy/var_1', lambdaLEVector_deg);

```

This script plot the graph after digitization. In this way it's possible to compare the initial graph and the digitized one.

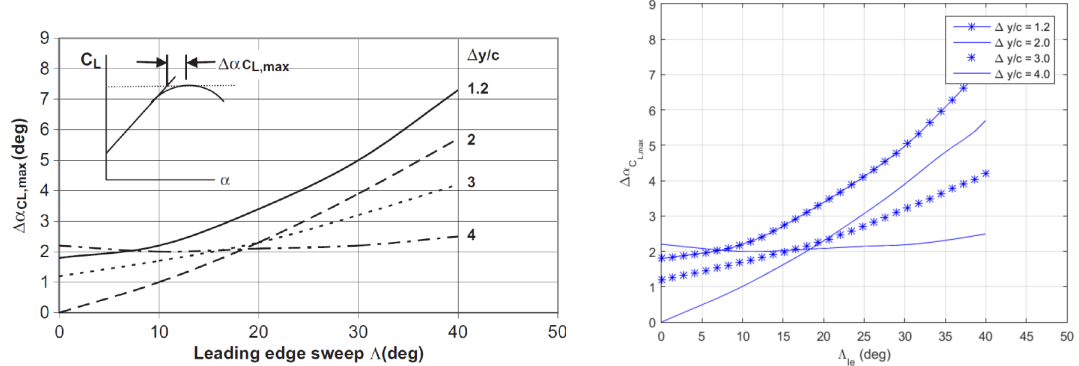


Figure A.2: Chart and its digitization.

Appendix B

App2

Glossary

Aircraft Construction Reference Frame The reference frame which has its origin in the fuselage forwardmost point, the x-axis pointing from the nose to the tail, the y-axis from fuselage plane of symmetry to the right wing (from the pilot's point of view) and the z-axis from pilot's feet to pilot's head.

client code the code where the code in question will be effectively exploited.

Graphical User Interface In computing, a Graphical User Interface is a type of interface that allows users to interact with electronic devices through graphical icons and visual indicators such as secondary notation, as opposed to text-based interfaces, typed command labels or text navigation.

List The `java.util.List` interface is a subtype of the `java.util.Collection` interface. It represents an ordered list of objects, meaning you can access the elements of a List in a specific order, and by an index too. You can also add the same element more than once to a List.

Map The `java.util.Map` interface represents a mapping between a key and a value. The Map interface is not a subtype of the Collection interface. Therefore it behaves a bit different from the rest of the collection types.

parsing Parsing or syntactic analysis is the process of analysing a string of symbols, either in natural language or in computer languages, conforming to the rules of a formal grammar.

reflection In computer science, reflection is the ability of a computer program to examine (see type introspection) and modify the structure and behavior (specifically the values, meta-data, properties and functions) of the program at runtime.

serialization In computer science, in the context of data storage, serialization is the process of translating data structures or object state into a format that can be stored (for example, in a file or memory buffer, or transmitted across a network connection link) and reconstructed later in the same or another computer environment.

Table a collection that associates an ordered pair of keys, called a row key and a column key, with a single value. A table may be sparse, with only a small fraction of row key / column key pairs possessing a corresponding value.

Unified Modeling Language The Unified Modeling Language (UML) is a general-purpose modeling language in the field of software engineering, which is designed to provide a standard way to visualize the design of a system.

user developer the term refers to the developer which will use a method without being interested in how the method performs the required action. This is the case of a utility method: the developer is the one who writes the method, while the user developer is who uses that method to accomplish some action which requires the functionality provided by the utility method. It has to be noticed that the user developer and the developer can be the same person.

wrapper function A wrapper function is a subroutine in a software library or a computer program whose main purpose is to call a second subroutine or a system call with little or no additional computation..

Acronyms

ACRF Aircraft Construction Reference Frame.

AIAA American Institute of Aeronautics and Astronautics.

BRF Body Reference Frame.

FAA Federal Aviation Administration.

GC Gravity Center.

GNC Guidance Navigation and Control.

GUI Graphical User Interface.

JPAD Java Aircraft Design.

MAC Mean Aerodynamic Chord.

MAPE Mean Absolute Percentage Error.

MLW Maximum Landing Weight.

MSL Mean Sea Level.

MTOW Maximum Take Off Weight.

MZFW Maximum Zero Fuel Weight.

UML Unified Modeling Language.

List of symbols

()_H quantity related to the horizontal tail.

()_{LG} quantity related to the landing gear.

()_N quantity related to the nacelle.

()_S quantity related to systems.

()_V quantity related to the vertical tail.

()_F quantity related to the fuselage.

()_{WF} quantity related to the wing-fuselage configuration.

D aerodynamic drag.

CG Center of Gravity.

\vec{g} gravitational acceleration.

i_H the angle between the horizontal tail root chord and the ACRF x-axis.

i_W the angle between the wing root chord and the ACRF x-axis.

L aerodynamic lift.

T Thrust.

M Mach number.

AR aspect ratio.

c chord.

d diameter.

l length.

m mass, in kg or lb.

n_{lim} limit load factor.

n_{ult} ultimate load factor.

b span.

S surface.

Λ sweep.

λ taper ratio.

t thickness.

V scalar velocity.

W weight, in Newtons.

m_w wing mass.

q dynamic pressure.

Re Reynolds number (evaluated with respect to \bar{c}).

α_w angolo d'attacco riferito alla corda di radice dell'ala.

β sideslip angle.

ρ air density.

Bibliography

- [1] I. H. Abbott and A. E. von Doenhoff. *Theory of Airfoil Sections*. Dover, 1959.
- [2] Joe Walnes et al. *XStream*. URL: <http://xstream.codehaus.org/>.
- [3] Guillaume Alleon. *occjava*. URL: <http://jcae.sourceforge.net/occjava.html>.
- [4] L. Attanasio. *Fuselage aerodynamic prediction methods*. Naples, 2015.
- [5] Various Authors. *ATR 72. Aircraft description*. URL: https://en.wikipedia.org/wiki/ATR_72.
- [6] Various Authors. *ATR 72. Aircraft description*. URL: <http://www.atraircraft.com/products/list.html>.
- [7] Various Authors. *Boeing 747. Aircraft description*. URL: https://en.wikipedia.org/wiki/Boeing_747.
- [8] Various Authors. *Boeing 747. Aircraft description*. URL: <http://www.boeing.com>.
- [9] Various Authors. *ESDU-76003. Geometrical properties of cranked and straight tapered wing planforms*. London, 2001.
- [10] Various Authors. *eXtensible Markup Language (XML)*. URL: <https://en.wikipedia.org/wiki/XML>.
- [11] Various Authors. *Guava*. URL: <https://github.com/google/guava>.
- [12] Various Authors. *JFace*. URL: <https://wiki.eclipse.org/JFace>.
- [13] Various Authors. *Model View Controller*. URL: <https://en.wikipedia.org/wiki/Model%C2%A2%C2%80%C2%93view%C3%A2%C2%80%C2%93controller>.
- [14] Various Authors. *Plot Digitizer, description*. URL: <http://plotdigitizer.sourceforge.net/>.
- [15] Various Authors. *The Lift Coefficient*. 2006. URL: <https://www.grc.nasa.gov/www/K-12/airplane/liftco.html>.
- [16] Various Authors. *The Standard Widget Toolkit*. URL: <https://www.eclipse.org/swt/>.
- [17] Various Authors. *Window Builder*. URL: <https://eclipse.org/windowbuilder/>.
- [18] Azeckoski. *ReflectUtils*. URL: <https://code.google.com/p/reflectutils/>.
- [19] A. et al. Bilgin. *Graphviz*. URL: <http://www.graphviz.org/>.
- [20] J. A. Jr Blackwell. *A Finite-Step Method for Calculation of Theoretical Load Distributions for Arbitrary Lifting-Surface Arrangements at Subsonic Speeds*. Washington, D.C., 1969.

- [21] AIR FORCE TEST PILOT SCHOOL EDWARDS AFB CA. *Volume II. Flying Qualities Phase. Chapter 5: Longitudinal Static Stability.* published by the author, OCT 1990.
- [22] M. Calcara. *Elementi di dinamica del velivolo.* Napoli: Edizioni CUEN, 1988. ISBN: 9788871460062. URL: <http://books.google.it/books?id=HqBoAQAAQACAAJ>.
- [23] Jean-Marie Dautelle. *Jscience.* URL: <http://jscience.org/>.
- [24] M. Drela and H. Youngren. *Xfoil, Subsonic Airfoil Development System.* 2008. URL: <http://web.mit.edu/drela/Public/web/xfoil/>.
- [25] Giuseppe Paduano Fabrizio Nicolosi. *BEHIND ADAS 1.0.* Napoli, 2011.
- [26] The Apache Software Foundation. *Apache Commons Math.* URL: <http://commons.apache.org/proper/commons-math/>.
- [27] The Apache Software Foundation. *Apache POI.* URL: <http://poi.apache.org/>.
- [28] The Apache Software Foundation. *Apache projects.* URL: <http://www.apache.org/>.
- [29] «Full-configuration drag estimation». In: *Journal of Aircraft* 47 (4) (2010).
- [30] D. Gambardella. «Development of a Java-Based Framework for Aircraft Preliminary Design». Master thesis. University of Naples "Federico II", 2014.
- [31] D. et al Gilbert. *JFreeChart.* URL: <http://www.jfree.org/jfreechart/>.
- [32] R.R Gilruth and M.D. White. *NACA TR 711 - Analysis And Prediction Of Longitudinal Stability of Airplanes.*
- [33] The HDF Group. *HDF.* URL: <http://www.hdfgroup.org/HDF5/>.
- [34] M. Hepperle. *Applet JavaFoil.* 2006. URL: <http://www.mh-aerotools.de/airfoils/javafoil.htm>.
- [35] W.F. Hilton. *High-speed Aerodynamics.* Longmans, Green, 1951. URL: https://books.google.it/books?id=%5C_RRFAAAAMAAJ.
- [36] D. E. Hoak et al. *The USAF Stability and Control DATCOM.* Tech. rep. (Revised 1978). 1960.
- [37] D. Howe. *Aircraft conceptual design synthesis.* Aerospace Series. Professional Engineering Publishing, 2000. ISBN: 9781860583018. URL: <https://books.google.it/books?id=QJZTAAAAMAAJ>.
- [38] D. Howe. *Aircraft Loading and Structural Layout.* AIAA Education Series, 2004.
- [39] J. Huwaldt. *1976 Standard Atmosphere Program.* URL: <http://thehuwaldtfamily.org/java/Applications/StdAtmosphere/StdAtmosphere.html>.
- [40] E. N. Jacobs and K. E. Ward. *Interference of wing and fuselage from tests of 209 combinations in the NACA variable-density tunnel.* Tech. rep. 1936.
- [41] L.R. Jenkinson, D. Rhodes, and P. Simpkin. *Civil jet aircraft design.* AIAA education series. Arnold, 1999. ISBN: 9780340741528. URL: <https://books.google.it/books?id=6tMeAQAAIAAJ>.
- [42] Erik K. Antonsson Karl-Heinrich Grote. *Springer Handbook of Mechanical Engineering.* Grote Antonsson.
- [43] K. Kawaguchi. *Args4j.* URL: <http://args4j.kohsuke.org/>.
- [44] I. Kroo and R. Shevell. *Aircraft Design: Synthesis and Analysis.* 1999.

- [45] Ajoy Kumar Kundu. *Aircraft Design*. Cambridge University Press, 2010.
- [46] S. Ledru and C. Denizet. *JLatexMath*. URL: <http://forge.scilab.org/index.php/p/jlatexmath/>.
- [47] W.H. Mason. «Analytic Models for Technology Integration in Aircraft Design». In: AIAA/AHS/ASEE (1990).
- [48] B. W. McCormick. *Aerodynamics, Aeronautics, and Flight Mechanics*. John Wiley & Sons, 1979.
- [49] H. Multhopp. *Aerodynamics of Fuselage*. 1942.
- [50] M. M. Munk. *Aerodynamic Forces of Airship Hulls*. Tech. rep. 1924.
- [51] Marcello R. Napolitano. *Aircraft Dynamics: From Modeling to Simulation*. John Wiley, 2012. ISBN: 9780470626672. URL: <http://www.amazon.com/Aircraft-Dynamics-From-Modeling-Simulation/dp/0470626674>.
- [52] R. Nelson. *Flight Stability and Automatic Control*. McGraw-Hill, 1989.
- [53] R.C. Nelson. *Flight Stability and Automatic Control*. Aerospace Science & Technology. McGraw-Hill International Editions, 1998. ISBN: 9780071158381. URL: <https://books.google.it/books?id=Uzs8PgAACAAJ>.
- [54] L.M. Nicolai and G. Carichner. *Fundamentals of Aircraft and Airship Design*. AIAA education series v. 1. American Institute of Aeronautics and Astronautics, 2010. ISBN: 9781600867514. URL: <https://books.google.it/books?id=qA0oAQAAQAAJ>.
- [55] M. Nita and D. Scholz. «Estimating Oswald Factor From Basic Aircraft Geometrical Parameters». In: *none* (2012).
- [56] E. Obert. *Aerodynamic Design of Transport Aircraft*. IOS Press, 2009. ISBN: 9781607504078. URL: <https://books.google.it/books?id=axPvAgAAQBAJ>.
- [57] C. D. Perkins and R. E. Hage. *Airplane Performance Stability and Control*. New York: John Wiley & Sons, 1949. ISBN: 9780471680468. URL: <https://books.google.it/books?id=DHxTAAAQAAJ>.
- [58] W. F. Phillips. «Lifting-Line Analysis for Twisted Wings and Washout-Optimized Wings». In: *Journal of Aircraft* Vol. 41.No. 1 (Jan.–Feb. 2004).
- [59] Warren F. Phillips. *Mechanics of Flight*. John Wiley and Sons, 2004. URL: https://books.google.it/books/about/Mechanics_of_Flight.html?id=6_iGbJHM-8C&redir_esc=y.
- [60] D.P. Raymer. *Aircraft Design: A Conceptual Approach*. 1992.
- [61] D.P. Raymer. *Aircraft Design / RDS-Student: A Conceptual Approach*. AIAA Education Series. Amer Inst of Aeronautics &, 2013. ISBN: 9781600869211. URL: <https://books.google.it/books?id=bvxllgEACAAJ>.
- [62] J. Roskam. *Airplane Design*. Airplane Design pt. 5. DARcorporation, 1999. ISBN: 9781884885501. URL: <https://books.google.it/books?id=mMU47Ld7yQkC>.
- [63] J. Roskam. *Airplane Design*. Airplane Design pt. 8. DARcorporation, 2002. ISBN: 9781884885556. URL: <https://books.google.it/books?id=GIHFkd829cC>.
- [64] J. Roskam. *Airplane Flight Dynamics and Automatic Flight Controls*. DARcorporation, 2001.

- [65] J. Roskam. *Airplane Flight Dynamics and Automatic Flight Controls*. Airplane Flight Dynamics and Automatic Flight Controls. Darcorporation, 2003. ISBN: 9781884885181. URL: <http://books.google.it/books?id=pWUAzy87zLYC>.
- [66] J. Roskam. *Methods for Estimating Stability and Control Derivatives of Conventional Subsonic Airplanes*. published by the author, 1971.
- [67] M.H. Sadraey. *Aircraft Design: A Systems Engineering Approach*. Aerospace Series. Wiley, 2012. ISBN: 9781118352809. URL: <https://books.google.it/books?id=VT-Tc3Tx5aEC>.
- [68] OPEN CASCADE S.A.S. *OpenCASCADE*. URL: <http://www.opencascade.org/>.
- [69] David Schmidt. *Modern Flight Dynamics*. McGraw-Hill, 2012. ISBN: 97800711339811.
- [70] P.M. Sforza. *Commercial Airplane Design Principles*. Elsevier Science, 2014. ISBN: 9780124199774. URL: <https://books.google.it/books?id=knhHAgAAQBAJ>.
- [71] Abe Silverstein and S. Katzoff. *Design Charts for Predicting Downwash Angles and Wake Characteristics behind Plain and Flapped Wings*. Tech. rep. 1939.
- [72] *Theoretical Calculation of the Effect of The Fuselage on the Spanwise Lift Distribution on a Wing*. Washington, D.C., 1952.
- [73] E. Torenbeek. *Advanced Aircraft Design: Conceptual Design, Technology and Optimization of Subsonic Civil Airplanes*. Aerospace Series. Wiley, 2013. ISBN: 9781118568095. URL: <https://books.google.it/books?id=C0gUyoYewhoC>.
- [74] E. Torenbeek. *Synthesis of Subsonic Aircraft Design*. 1976.
- [75] E. Torenbeek. *Synthesis of Subsonic Airplane Design: An Introduction to the Preliminary Design of Subsonic General Aviation and Transport Aircraft, with Emphasis on Layout, Aerodynamic Design, Propulsion and Performance*. Springer, 1982. ISBN: 9789024727247. URL: https://books.google.it/books?id=NG2%5C_qiSjmMEC.
- [76] Dimitri Van Heesch. *Doxygen*. 1997-2014. URL: www.doxygen.org.
- [77] S. R. Vukelich and J. E. Williams. *The USAF Stability and Control Digital Datcom*. AFFDL-TR-79-3032. Updated by Public Domain Aeronautical Software 1999. Apr. 1979. Volume I.
- [78] A.D. Young. *The Aerodynamic Characteristics of Flaps*. Technical Report. 1947.